Available free online at www.medjchem.com

Mediterranean Journal of Chemistry

Mediterranean Journal of Chemistry **2023**, 13(3), 188-209

Transition metal complexes of 1-(1-hydroxypropan-2-ylidene) thiosemicarbazide (H_2L): Synthesis, spectroscopic study, and X-ray diffraction structures

Binta Diom [1], Cheikh Ndoye [1], Thierno Moussa Seck [1], Bocar Traore [1], Ousmane Diouf [1], Grégory Excoffier [2], and Mohamed Gaye [1,*]

[1] Department of Chemistry, University Cheikh Anta Diop, Dakar, 10700, Sénégal

[2] Aix Marseille Univ, CNRS, Centrale Marseille, FSCM, Spectropole, Marseille, France.

Abstract: A series of metal complexes of one Co(II), three Ni(II), one Cu(II), and one Zn(II) with (1-(1-hydroxypropan-2-ylidene) thiosemicarbazide (H_2L) have been synthesized and successfully characterized using various spectroscopic methods. A single X-ray diffraction technic determined the complexes' molecular structures. The ligand which acts in tridentate fashion afforded complexes formulated respectively as $[Co(H_2L)_2](NO_3)_2$ (**1**), $[Ni(H_2L)_2](ClO_4)_2{\cdot}2H_2O$ (**2**), $[Ni(H_2L)_2](NO_3)_2$ (**3**), $[Ni(HL)(H_2L)](NO_3){\cdot}0.75(H_2O)$ (**4**), $[Cu(H_2L)Cl](Cl){\cdot}0.5H_2O$ (**5**), and $[Zn(H_2L)_2](ClO_4)_2{\cdot}2H_2O$ (**6**). These compounds have been studied and characterized by elemental analysis, IR and UV-Vis spectroscopies, molar conductivity, and room-temperature magnetic measurements. The structures of the six complexes have been resolved by X-ray crystallography technique. The asymmetric unit of complex **1** contains two mononuclear cationic units in which the two ligand molecules of each unit act in their neutral forms in a tridentate fashion. In the mononuclear complexes **2**, **3,** and **6**, the asymmetric units contain one cationic unit in which the two ligand molecules act in neutral forms in -η^3 modes. In complex **4**, the asymmetric unit has one cationic unit in which one ligand molecule acts in a tridentate fashion in its neutral form. In contrast, the second ligand molecule acts tridentate in its mono-deprotonated form. In complex **5**, the asymmetric unit contains one complex molecule in which the copper(II) ion is linked to one neutral ligand molecule in -η^3 mode and two terminal chloride anions. In complexes (**1**-**4**) and (**6**), the environments around the metal are best described as octahedral geometries. In contrast, the environment around the Cu(II) in complex (**5**) is best described as a square planar geometry. Hydrogen bonds consolidated the structures of all the complexes.

Keywords: Thiosemicarbazide; Schiff base; Spectroscopy; Complex; Octahedral.

1. Introduction:

The condensation reaction between thiosemicarbazide and a carbonyl compound obtains the Schiff bases containing semicarbazone or thiosemicarbazone moieties. These compounds have been extensively studied due to their interesting biological properties, analytical applications, and exciting chemical and structural properties of metal ions [1–6]. They possess a wide spectrum of biological activities such as antioxidant [7,8], antitumor [8,9], antituberculosis [10,11], antifungal [10,12], antibacterial [10,13], analgesic [14], antiviral, and antimalarial [1,2]. In search of potential antitumor drug candidates, a series of thiosemicarbazide ligands obtained by the addition of 4-(2-pyridyl)-3-thiosemicarbazide with (phenyl and benzoyl) isothiocyanate and phenyl isocyanate has been reported in the literature. Interesting physical properties are reported when the Schiff bases ligand derived from thiosemicarbazide are combined with metal ions [15–17]. Transition metals and lanthanide complexes have been reported in the literature because of their physical properties such as magnetism [18–20], fluorescence [21–23] or catalytic [24–26].

In this context, we report the synthesis and structural characterization of the Ni(II), Co(II), and Zn(II) complexes derived from 1-(1-hydroxypropan-2-ylidene)thiosemicarbazide (H_2L, Fig. 1). The ligand has been fully characterized using NMR and IR spectroscopies, and elemental analysis. In addition, the complexes have been studied and described by infrared, ultraviolet-visible (UV-Vis) spectroscopies, conductivity, and magnetic susceptibility at low temperatures. X-ray diffraction analysis also reports the molecular structures of the complexes and the thiosemicarbazone ligand (H_2L, Fig. 1).

2. Experimental section

2.1. Material and procedures

Thiosemicarbazide, 1-hydroxyacetone, zinc (II)

**Corresponding author: Mohamed Gaye*
Email address: mohamedl.gaye@ucad.edu.sn
DOI: http://dx.doi.org/10.13171/mjc02305201688gaye

Received February 6, 2023
Accepted May 1, 2023
Published May 20, 2023

perchlorate hexahydrate, nickel (II) perchlorate hexahydrate, nickel (II) nitrate hexahydrate, and cobalt (II) nitrate hexahydrate were purchased from Sigma-Aldrich and used as received without further purification. The solvents were reagent grade and were purified by usual methods. Elemental analyses of C, H, and N were recorded on a Vario EL Instrument. The IR spectra were recorded on an FTIR Spectrum Two of Perkin Elmer (4000–400 cm^{-1}). The UV–Vis spectra were run on a Perkin-Elmer UV/Visible spectrophotometer Lambda 365 (1000–200 nm). The Schiff base's 1H and 13C NMR spectra were recorded in DMSO-d_6 on a BRUKER 500 MHz spectrometer at room temperature using TMS as an internal reference. The molar conductance of 10^{-3} M solutions of the metal complexes in DMF was measured at 25°C using a WTW LF-330 conductivity meter with a WTW conductivity cell. Magnetic measurements for complexes were performed at room temperature by using a Johnson Mattey scientific magnetic susceptibility balance (Calibrant: $Hg[Co(SCN)_4]$).

2.2. Synthesis of ligand 1-(1-hydroxypropan-2-ylidene) thiosemicarbazide (H_2L)

The compound H_2L is synthesized using the method reported by Netalkar *et al.* [27] with a slight modification. In a 250 mL flask containing 30 mL of methanol, 0.0219 mol (2 g) was introduced. A methanol solution containing 0.0219 mol (1.503 mL) of 1-hydroxyacetone was added, and the mixture was refluxed for 4 hours. On cooling, the beige solution gives a white residue, which is recovered by filtration, washed with 2×20 mL of methanol, then 20 ml of diethyl ether, and dried in a desiccator. Yield: 80 %. m.p: 175-176 °C. FT-IR (KBr, ν, cm^{-1}): 3380, 3217, 3164, 3139, 3031, 1603, 1538, 1453, 1449, 1400, 1372, 1311, 1258, 1116, 1068, 1056, 985, 879, 791, 721, 627, 536, 498. ^{1}H NMR (500 MHz, DMSO-d_6, δ, ppm): 10.01 (s, 1H, NH), 7.90-8.06 (s, 2H, NH_2), 4.88 (s, 1H, OH), 4.01 (s, 2H, -CH_2-OH), 1.87 (S, 3H, -CH_3). ^{13}CNMR (125 MHz, DMSO-*d*6, δ, ppm): 14.15 (-CH_3), 65.36 (-CH_2-OH), 153.08 (C=N), 179.54 (C=S). Anal. calc. for $C_4H_9N_3OS$: C, 32.64; H, 6.16; N, 28.55 %. Found: C, 32.61; H, 6.14; N, 28.51%. UV-Vis (λ_{max}, nm): 277.

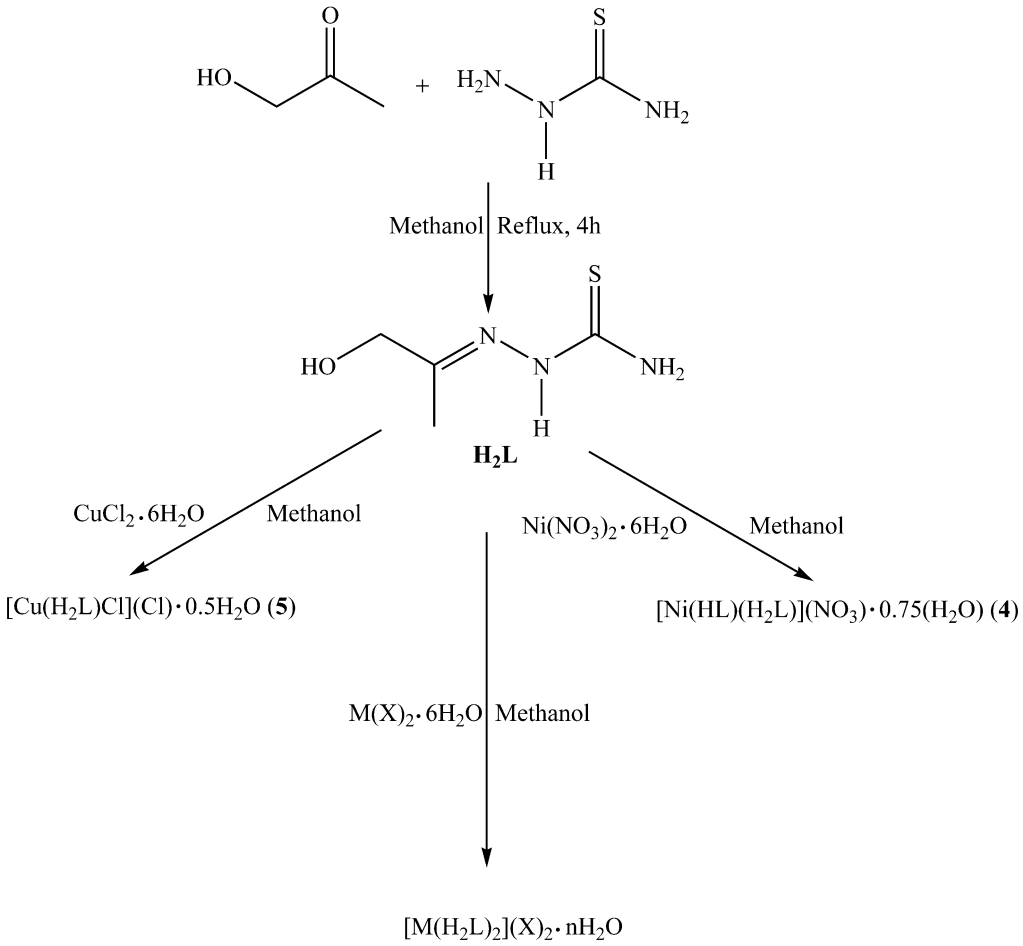

M = Co, X = NO_3^-, n = 0 (**1**); M = Ni, X = ClO_4^-, n = 2 (**2**);

M = Ni, X = NO_3^-, n = 0 (**3**); M = Zn, X = ClO_4^-, n = 2 (**6**).

Figure 1. Synthetic route of H_2L and its metal transition complexes

2.3. Synthesis of the complex $[Co(H_2L)_2](NO_3)_2$ (1)

To a methanolic solution (10 mL) of the ligand H_2L 0.148 g (1 mmol), a solution of the $Co(NO_3)_2{\cdot}6H_2O$ 0.291 g (1 mmol) in methanol (10 mL) was added. The obtained solution was stirred at room temperature for one hour and then filtered. The brown filtrate was left to slow evaporation, and brown crystals suitable for X-ray analysis were formed after one week. Yield 61.4 %. Anal. Calc for $C_{16}H_{36}Co_2N_{16}O_{16}S_4$: C, 20.13; H, 3.80; N, 23.47; S,13.43 %. Found: C, 20.11; H, 3.69; N, 23.44; S, 13.41 %. IR (cm^{-1}): 3378 (OH), 3308 (NH_2), 3158 (N-H), 1607 (C=N), 1380 (NO_3), 1228 (C=S), 1035 (C-O). UV–Vis (λmax, DMF solution, nm): 225, 298, 402, 532, 1080. Λ (Ω^{-1} cm^2 mol^{-1}): 135 (fresh solution) and 165 (two weeks after). μ_{eff} = 5.9 μ_B.

2.4. Synthesis of the complex $[Ni(H_2L)_2](ClO_4)_2{\cdot}2H_2O$ (2)

The procedure used for the synthesis of (**1**) was used: $Ni(ClO_4)_2{\cdot}6H_2O$ 0.363 g (1 mmol) instead of $Co(NO_3)_2.6H_2O$. The green filtrate was left to slow evaporation, and green crystals suitable for X-ray analysis were formed after seven days. Yield 89.3 %. Anal. Calc for $C_8H_{22}Cl_2N_6NiO_{12}S_2$: C, 16.34; H, 3.77; N, 14.29; Cl, 12.06; S, 10.91 %. Found: C, 16.31; H, 3.75; N, 14.26; Cl, 12.03; S, 10.88 %. IR (cm^{-1}): 3400 (OH), 3300 (NH_2), 3153 (N-H), 1612 (C=N), 1230 (C=S), 1049 (C-O), 1070 and 620 (ClO_4). UV–Vis (λmax, DMF solution, nm): 227, 295, 405, 544, 880. Λ ($\Omega^{-1}cm^2mol^{-1}$): 155 (fresh solution) and 165 (two weeks after). μ_{eff} = 3.37 μ_B.

2.5. Synthesis of the complex $[Ni(H_2L)_2](NO_3)_2$ (3) and $[Ni(HL)(H_2L)](NO_3){\cdot}0.75(H_2O)$ (4)

The procedure used for the synthesis of (**1**) was used: $Ni(NO_3)_2{\cdot}6H_2O$ 0.290 g (1 mmol) instead $Co(NO_3)_2.6H_2O$. The green filtrate was left to slow evaporation, and two types of green crystals suitable for X-ray diffraction were formed after 5 days.

(**3**) : Yield 38.3 %. Anal. Calc. for $C_8H_{18}N_8NiO_8S_2$: C, 20.14; H, 3.80; N, 23.49; S, 13.44 %. Found: C, 20.12; H, 3.77; N, 23.47; S, 13.41 %. IR (cm^{-1}): 3354 (OH), 3256 (NH_2), 3154 (N-H), 1639 (C=N), 1380 (NO_3), 1238 (C=S), 1048 (C-O). UV–Vis (λmax, DMF solution, nm): 228, 296, 395, 402, 550, 771 (large). Λ (Ω^{-1} cm^2 mol^{-1}): 150 (fresh solution) and 170 (two weeks after). μ_{eff} = 3.46 μ_B.

(4) : Yield 38.9 %. Anal. Calc. for $NiC_8H_{18.5}N_7O_{5.75}S_2$: C, 22.47; H, 4.36; N, 22.93; S, 15.00 %. Found: C: 22.45; H, 4.33; N, 22.90; S, 14.97 %. IR (cm^{-1}): 3350 (OH), 3251 (NH_2), 3148 (N-H), 1634 (C=N), 1380 (NO_3), 1238 (C=S), 1040 (C-O). UV–Vis (λmax, DMF solution, nm): 228, 295, 392, 403, 540, 770 (large). Λ (Ω^{-1} cm^2 mol^{-1}): 65 (fresh solution) and 75 (two weeks after). μ_{eff} = 3.49 μ_B.

2.6. Synthesis of the complex $[Cu(H_2L)Cl](Cl){\cdot}0.5H_2O$ (5)

The procedure used for the synthesis of (**1**) was used: $CuCl_2{\cdot}6H_2O$ 0.17048 g (1 mmol) instead of $Co(NO_3)_2.6H_2O$. The green filtrate was left to slow evaporation, and green crystals suitable for X-ray analysis were formed after one week. Yield 86.7 %. Anal. Calc for $C_4H_{10}Cl_2CuN_3O_{1.5}S$: C, 16.53; H, 3.47; N, 14.46; S, 11.03 %. Found: C, 16.50; H, 3.44; N, 14.49; S, 11.00 %. IR (cm^{-1}): 3402 (OH), 3310 (NH_2), 3160 (N-H), 1593 (C=N), 1246 (C=S), 1105 (C-O). UV–Vis (λmax, DMF solution, nm): 227, 298, 398, 407, 591. Λ (Ω^{-1} cm^2 mol^{-1}): 65.7 (fresh solution) and 67.8 (two weeks after). μ_{eff} = 1.69 μ_B.

2.7. Synthesis of the complex $[Zn(H_2L)_2](ClO_4)_2{\cdot}2H_2O$ (6)

The procedure used for the synthesis of (**1**) was used: $Zn(ClO_4)_2{\cdot}6H_2O$ 0.370 g (1 mmol) instead of $Co(NO_3)_2{\cdot}6H_2O$. The filtrate was left to slow evaporation, and yellow crystals suitable for X-ray analysis were formed after a few days. Yield 73.1 %. Anal. Calc for $C_8H_{22}Cl_2N_6O_{12}S_2Zn$: C, 16.16; H, 3.73; N, 14.13; Cl, 11.92; S, 10.78 %. Found: C, 16.14; H, 3.71; N, 14.10; Cl, 11.989; S, 10.76 %. IR (cm^{-1}): 3357(OH), 3252 (NH_2), 3155 (N-H), 1592 (C=N), 1252 (C=S), 1045 (C-O), 1069 and 619 (ClO_4. UV–Vis (λmax, DMF solution, nm): 225, 302, 398, 405. Λ (Ω^{-1} cm^2 mol^{-1}): 135 (fresh solution) and 143 (two weeks after).

2.8. X-ray data collection, structure determination, and refinement

Single crystals **1**, **2**, and **3** were grown by slow evaporation of the methanol solution of the corresponding complex. Suitable crystals were selected and mounted on a Rigaku Oxford Diffraction Super Nova diffractometer at the MoKα radiation for compounds **1** and at the CuKα radiation for compounds **2, 3, and 4**. The crystallographic details of compounds **1-6** are summarized in Table 1. Using *Olex2* [28], the structure was solved with the *SHELXT* [29] structure solution program using direct methods and refined with the *SHELXL* [30] refinement package. Molecular graphics were generated using *ORTEP*-3 [31].

Additional material from the Cambridge Crystallographic Data Center comprises thermal parameters and remaining bond distances and angles (CCDC No. 2237952 (**1**), 2237949 (**2**), 2237953 (**3**), 2237950 (**4**), 2237951 (**5**), 2237948 (**6**)). These data can be obtained free of charge from The Cambridge Crystallographic Data Center (CCDC), 12 Union Road, Cambridge CB2 IEZ, UK (fax +44(0)1223-336033; e-mail: deposit@ccdc.cam.ac.UK).

Table 1. Crystal data and structure refinement for 1, 2, 3, 4, 5 and 6.

Chemical formula	$(C_8H_{18}N_6O_2S_2Co)(NO_3)_2$ (**1**)	$(C_8H_{18}N_6O_2S_2Ni)(ClO_4)_2\cdot 2(H_2O)$ (**2**)	$(C_8H_{18}N_6O_2S_2Ni)(NO_3)_2$ (**3**)	$(C_8H_{17}N_6O_2S_2Ni)(NO_3)\cdot 0.75(H_2O)$ (**4**)	$(C_4H_9ClN_3OSCu)(Cl)\cdot 0.5(H_2O$ (**5**)	$(C_8H_{18}N_6O_2S_2Zn)(ClO_4)_2\cdot 2(H_2O)$ (**6**)
*M*r	477.35	588.04	477.13	427.63	290.65	590.67
Crystal system	Triclinic	Triclinic	Monoclinic	Triclinic	Monoclinic	Monoclinic
Space group	P$\bar{1}$	P$\bar{1}$	*C*2/*c*	P$\bar{1}$	*C*2/*c*	*C*2/*c*
Temperature (K)	295	100	295	295	298	295
a (Å)	10.3804(4)	8.8727(1)	19.7378(7)	7.9088(1)	14.2234(3)	11.6585 (2)
b (Å)	13.9213(8)	9.0916(2)	7.0598(3)	10.4179(2)	9.4153(2)	12.6963 (2)
c (Å)	13.9663(6)	13.305(2)	13.0908(6)	10.7762(2)	15.4526(3)	16.2641 (3)
α (°)	89.978(4)	86.386(1)	-	81.872(2)	-	-
β (°)	70.313(4)	81.391(1)	94.972(3)	83.565(1)	92.811(2)	108.804 (2)
γ (°)	82.784(4)	85.498(1)	-	76.729(2)	-	-
V (Å^3)	1883.33(16)	1060.09(3)	1817.27(13)	852.57(3)	2066.88(7)	2278.92 (7)
Z	4	2	4	2	8	4
Radiation type	Mo *K*α	Mo *K*α	Mo *K*α	Cu *K*α	Mo *K*α	Cu *K*α
μ (mm^{-1})	1.19	1.43	1.36	4.31	2.80	5.99
Crystal size (mm)	0.26 × 0.16 × 0.11	0.17 × 0.07 × 0.06	0.50 × 0.20 × 0.08	0.28 × 0.17 × 0.10	0.12 × 0.12 × 0.05	0.19 × 0.13 × 0.05
T_{min}, T_{max}	0.888, 1.000	0.631, 1.000	0.520, 1.000	0.673, 1.000	0.799, 1.000	0.525, 1.000
No. of measured reflections	19381	29887	9590	24294	15840	7364
No. of independent reflections	8164	5466	2096	3343	2301	2193
No. of observed [$I > 2\sigma(I)$] reflections	3404	4955	1836	3120	2059	2021
R_{int}	0.024	0.031	0.035	0.036	0.027	0.039
$R[F^2 > 2\sigma(F^2)]$	0.045	0.029	0.037	0.029	0.028	0.057
$wR(F^2)$	0.168	0.085	0.094	0.079	0.078	0.177
S	1.04	1.07	1.05	1.04	1.07	1.08
No. of parameters	503	297	127	225	122	149
No. of restraints	12	0	3	6	3	3
$\Delta\rho_{max}$, $\Delta\rho_{min}$ (e Å^{-3})	0.44, -0.31	0.79, -0.92	0.63, -0.45	0.32, -0.35	0.67, -0.27	0.77, −0.57

3. Results and Discussion

3.1. Crystal structure of $[Co(H_2L)_2](NO_3)_2$ (1)

The compound crystallizes in the triclinic system with the space group of Pī. The selected bond distances and angles are listed in Table 2, and the ORTEP representation of the structure is illustrated in Fig. 2. The asymmetric unit contains two Co^{2+} cations, four non-deprotonated ligands, and four uncoordinated nitrate anions. Two ligand molecules coordinate each Co^{2+} cation through their azomethine nitrogen atoms, alcoholic oxygen atoms, and thione sulfur atoms resulting in an $N_2O_2S_2$ core. The environment of each hexacoordinated cobalt cation is best described by an octahedral geometry in which the basal plane is occupied by two azomethine nitrogen atoms, one thione sulfur atom, and one alcoholic oxygen atom (N3, N6, S1, and O1 for Co1; N9, N12, S3, and O4 for Co2) and the apical positions being occupied by one thione sulfur atom and one alcoholic oxygen atom (S2 and O2 for Co1; S4 and O3 for Co2). The *transoid* angles are S1—Co1—O1 = 154.50(11)°, (N3—Co1—N6 = 156.63(13)°, S3—Co2—O4 = 154.42(12)° and N9—Co2—N12 = 156.74(14)°. The *cissoid* angles in the basal planes are in the range [74.08(13)°-116.25(11)°]. The angles subtended by the atoms in apical positions are S2—Co1—O2 = 157.37(11)° and S4—Co2—O3 = 154.43(10)°. The values of these angles deviate severely from the ideal values of 90° and 180° expected for a perfect octahedral geometry. The geometry around the hexacoordinated Co1 and Co2 is strongly distorted. In each Co, the two coordinated ligands are quite planar (RMS 0.058 and 0.0566 (Co1); 0.0793 and 0.3333 (Co2)) and for form dihedral angle of 80.248(6)° (Co1) and 72.914()° (Co2). The distances Co—S, Co—N, and Co—O falls in the range [2.4252(14) Å-2.4278(14) Å], [2.077(3) Å -2.088(2) Å] and [2.097(3) Å -2.113(3) Å] respectively and agree with the values reported for similar compounds [32–34].

Each mononuclear Co(II) molecule complex is connected to another complex molecule by hydrogen bonding interactions leading to the formation of a supramolecular chain structure propagating along the *a* axis. The chains are connected by hydrogen bonding interaction of type N—H···O, O—H···O, and O—H···N. The uncoordinated nitrate anion act via hydrogen bonds as a bridge between the chains, leading to a 3D supramolecular structure (Fig. 3, Table 3).

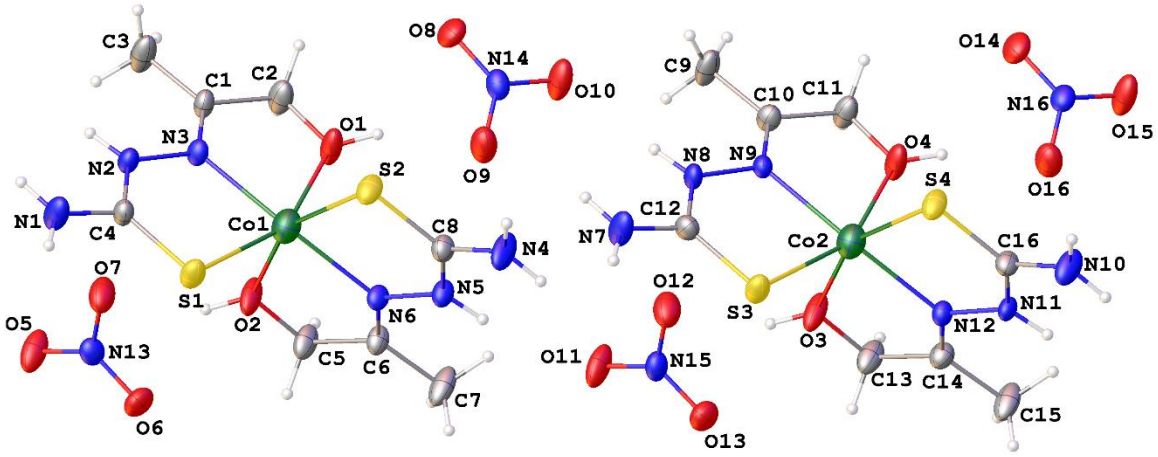

Figure 2. ORTEP view of compound **1**

Table 2. Selected geometric parameters (Å, °).

Atoms	Distance	Atoms	Distance
Co1—S1	2.4275 (14)	Co2—S3	2.4257 (13)
Co1—S2	2.4252 (14)	Co2—S4	2.4278 (14)
Co1—N3	2.077 (3)	Co2—N12	2.082 (3)
Co1—N6	2.083 (3)	Co2—N9	2.088 (3)
Co1—O1	2.113 (3)	Co2—O3	2.110 (3)
Co1—O2	2.109 (3)	Co2—O4	2.097 (3)
Atoms	**Angle**	**Atoms**	**Angle**
S2—Co1—S1	90.73 (5)	S3—Co2—S4	90.82 (5)

N3—Co1—S1	80.86 (10)	N12—Co2—S3	116.00 (10)
N3—Co1—S2	116.42 (11)	N12—Co2—S4	81.05 (11)
N3—Co1—N6	156.63 (13)	N12—Co2—N9	156.74 (14)
N3—Co1—O1	74.35 (13)	N12—Co2—O3	74.12 (14)
N3—Co1—O2	89.18 (15)	N12—Co2—O4	89.56 (14)
N6—Co1—S1	116.25 (11)	N9—Co2—S3	81.06 (10)
N6—Co1—S2	80.84 (10)	N9—Co2—S4	116.02 (10)
N6—Co1—O1	89.23 (14)	N9—Co2—O3	89.52 (14)
N6—Co1—O2	74.23 (13)	N9—Co2—O4	74.08 (13)
O1—Co1—S1	154.50 (11)	O3—Co2—S3	94.54 (13)
O1—Co1—S2	94.89 (13)	O3—Co2—S4	154.43 (10)
O2—Co1—S1	94.92 (13)	O4—Co2—S3	154.42 (10)
O2—Co1—S2	154.37 (11)	O4—Co2—S4	94.63 (13)
O2—Co1—O1	90.70 (19)	O4—Co2—O3	91.24 (19)

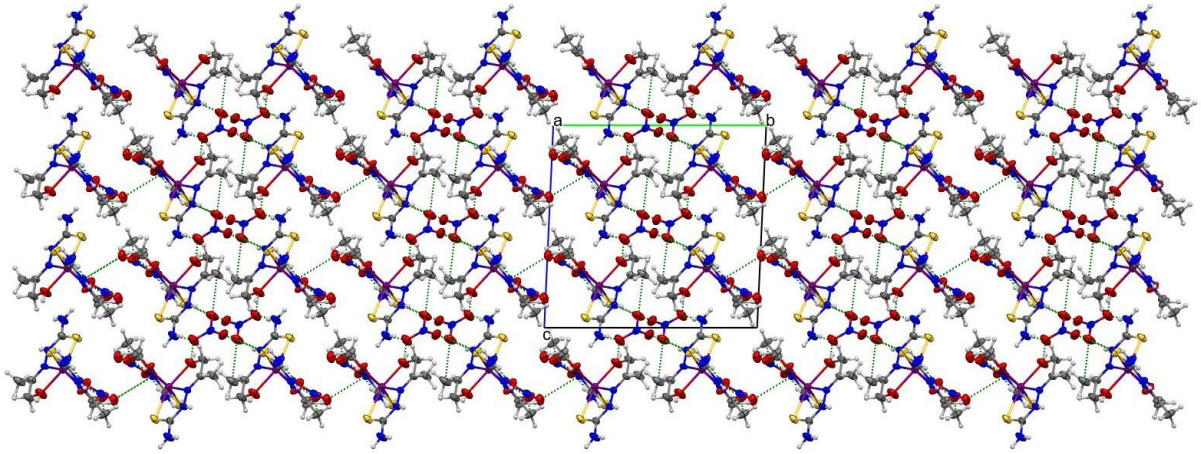

Figure 3. Crystal packing observed in compound **1**

Table 3. Hydrogen-bond geometry (Å, °).

D—H···*A*	*D*—H	H···*A*	*D*···*A*	*D*—H···*A*
N11—H11···O11^{i}	0.86	2.06	2.896 (5)	165.1
N8—H8···O10	0.86	2.07	2.907 (5)	164.5
N5—H5···O5^{i}	0.86	2.06	2.901 (5)	164.9
O3—H3···O13	0.857 (9)	2.396 (18)	3.115 (5)	142 (2)
O3—H3···N15	0.857 (9)	2.477 (13)	3.317 (6)	166 (3)

O3—H3···O12	0.857 (9)	1.912 (19)	2.725 (5)	158 (5)
N2—H2···O15^{ii}	0.86	2.06	2.898 (5)	165.8
O4—H4···N16	0.853 (9)	2.493 (14)	3.324 (6)	165 (3)
O4—H4···O14	0.853 (9)	2.46 (2)	3.139 (5)	137 (3)
O4—H4···O16	0.853 (9)	1.903 (11)	2.736 (5)	165 (2)
O1—H1···O8	0.854 (9)	2.423 (19)	3.127 (5)	140 (2)
O1—H1···N14	0.854 (9)	2.469 (12)	3.302 (5)	165 (3)
O1—H1···O9	0.854 (9)	1.905 (18)	2.721 (5)	159 (4)
O2—H2A···O6	0.858 (9)	2.427 (17)	3.140 (5)	141 (2)
O2—H2A···O7	0.858 (9)	1.92 (2)	2.735 (5)	157 (5)
O2—H2A···N13	0.858 (9)	2.484 (14)	3.318 (6)	164 (3)
N7—H7D···O9	0.86	2.07	2.913 (6)	166.3
N7—H7E···O7^{i}	0.86	2.54	3.348 (6)	156.1
N7—H7E···N13^{i}	0.86	2.69	3.493 (6)	156.3
N7—H7E···O5^{i}	0.86	2.44	3.206 (7)	148.7
N1—H1A···O16^{ii}	0.86	2.07	2.913 (6)	166.0
N1—H1B···N15^{iii}	0.86	2.68	3.488 (6)	156.6
N1—H1B···O12^{iii}	0.86	2.55	3.352 (6)	155.8
N1—H1B···O11^{iii}	0.86	2.44	3.210 (7)	149.1
N4—H4A···O7^{i}	0.86	2.08	2.924 (5)	166.8
N4—H4B···N16^{iii}	0.86	2.69	3.498 (6)	157.3
N4—H4B···O15^{iii}	0.86	2.44	3.211 (7)	149.3
N4—H4B···O16^{iii}	0.86	2.53	3.331 (6)	156.3
N10—H10A···O12^{i}	0.86	2.08	2.918 (5)	165.8
N10—H10B···N14^{i}	0.86	2.67	3.479 (6)	156.7
N10—H10B···O9^{i}	0.86	2.55	3.351 (6)	156.2
N10—H10B···O10^{i}	0.86	2.45	3.223 (7)	149.1

3.2. Crystal structure of $[Ni(H_2L)_2](ClO_4)_2{\cdot}2H_2O$ (2)

The hexacoordinated Ni(II) compound **2** crystallizes with the space group Pī in the triclinic system. The selected bond distances and angles are listed in Table 4, and the *ORTEP* representation of **2** is shown in Fig. 4. The asymmetric unit of the crystal structure of compound **2** contains one $[Ni(H_2L)_2]^{2+}$, two uncoordinated perchlorate anions ClO_4^{-}, and two free water molecules. The two ligand molecules act tridentate through the azomethine nitrogen atom, the sulfur atom, and the alcoholic oxygen atom. Thus,

the Ni^{2+} cation is situated in an $N_2O_2S_2$ inner, and its coordination sphere is best described as a severely distorted octahedral polyhedron. The equatorial plane is occupied by the two sulfur atoms and the two oxygen atoms of the ligand. The two imino nitrogen atom occupies the axial positions with 168.01(6)° [N1—Ni1—N4]. The *cissoid* angle values in the equatorial plane are in the range [85.93 (5)°—97.473 (18)°] with the sum value of the angles of 356.43°. The *transoid* angles values are O1—Ni1—S1 = 159.24 (4)° and O2—Ni1—S2 = 160.45 (4)°. These values deviate severely from the ideal values, indicating strong distortion from the ideal octahedral geometry. These angle values are comparable to those of a similar compound $[Ni(H_2L)_2]\cdot[(SCN)_2$. Each h^3-H_2L forms two five-membered rings of type NiSCNN and NiOCCN with bite angles of 84.11 (4)° and 75.57 (5)° for one ligand and 83.53 (4)° and 77.40 (6)° for the second ligand. In each ligand, the two five-membered rings are almost planar NiSCNN (rms: 0.0462 Å and 0.0173 Å) and NiOCCN (rms: 0.1098 Å and 0.0647 Å). The two five-membered rings relative to the ligand are twisted and form dihedral angles of 7.875 (1)° and 3.143 (1)°. The mean planes of the two ligand molecules around the Ni1 ions are quite perpendicular with a dihedral angle of 83.520 (1)°. The Ni—S distances [2.3748(5) Å and 2.3846(5) Å] and the C—S distances [1.6985(18) Å and 1.6985(18) Å] indicate clearly that the compound acts in its thione form [35]. The Ni—O distances [2.1530(13) Å and 2.1587(13) Å] are comparable to the analogous bond reported for compound [36]. The perchlorate anions are tetrahedral, and one oxygen atom of one of the perchlorate anions is disordered, with two sites having occupancies of 0.25 and 0.75.

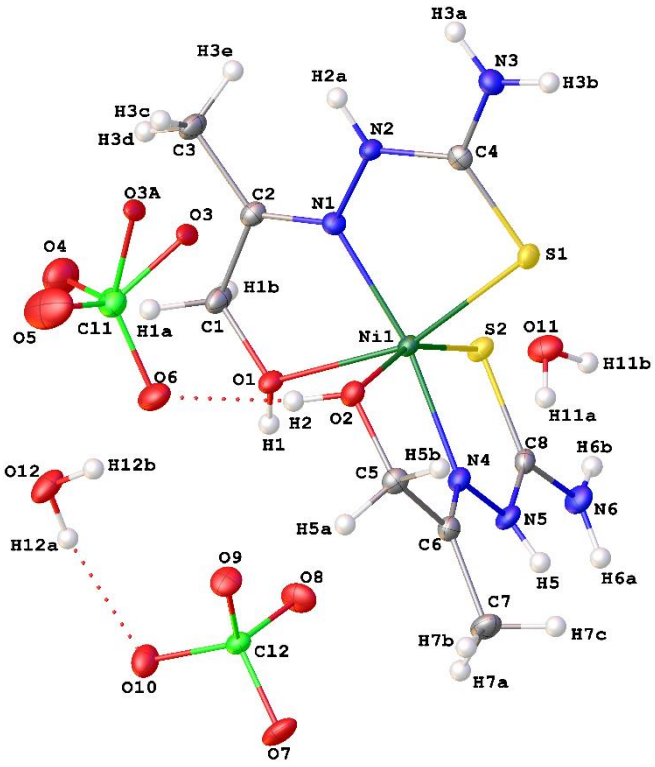

Figure 4. ORTEP view of the compound **2**

Table 4. Selected geometric parameters (Å, °).

Atoms	Distance	Atoms	Distance
Ni1—S2	2.3846 (5)	Ni1—N1	2.0133 (15)
Ni1—S1	2.3748 (5)	S2—C8	1.6985 (18)
Ni1—O2	2.1587 (13)	S1—C4	1.6977 (18)
Ni1—O1	2.1530 (13)	O2—C5	1.428 (2)
Ni1—N4	2.0152 (15)	O1—C1	1.435 (2)
Atoms	**Angle**	**Atoms**	**Angle**

S1—Ni1—S2	97.473 (18)	N4—Ni1—O2	77.40 (6)
O2—Ni1—S2	160.45 (4)	N4—Ni1—O1	96.98 (5)
O2—Ni1—S1	90.83 (4)	N1—Ni1—S2	105.85 (4)
O1—Ni1—S2	92.19 (4)	N1—Ni1—S1	84.11 (4)
O1—Ni1—S1	159.24 (4)	N1—Ni1—O2	92.54 (5)
O1—Ni1—O2	85.93 (5)	N1—Ni1—O1	75.57 (5)
N4—Ni1—S2	83.53 (4)	N1—Ni1—N4	168.01 (6)
N4—Ni1—S1	102.32 (4)		

Table 5. Hydrogen-bond geometry (Å, °).

D—H···*A*	*D*—H	H···*A*	*D*···*A*	*D*—H···*A*
O2—H2···O6	0.84	1.98	2.797 (2)	163.9
O1—H1···O10^{i}	0.84	2.08	2.8348 (19)	148.5
O11—H11A···O6^{ii}	0.87	2.02	2.876 (2)	166.5
O11—H11B···O5^{iii}	0.87	2.10	2.881 (2)	149.0
O12—H12A···O10	0.87	2.05	2.884 (2)	159.1
N2—H2A···O11^{iv}	0.88	1.98	2.805 (2)	155.3
N5—H5···O12^{iii}	0.78 (3)	2.00 (3)	2.742 (2)	159 (3)

Symmetry codes: (i) −x+1, −y, −z+1; (ii) −x+1, −y, −z+2; (iii) x+1, y, z; (iv) −x+1, −y+1, −z+2.

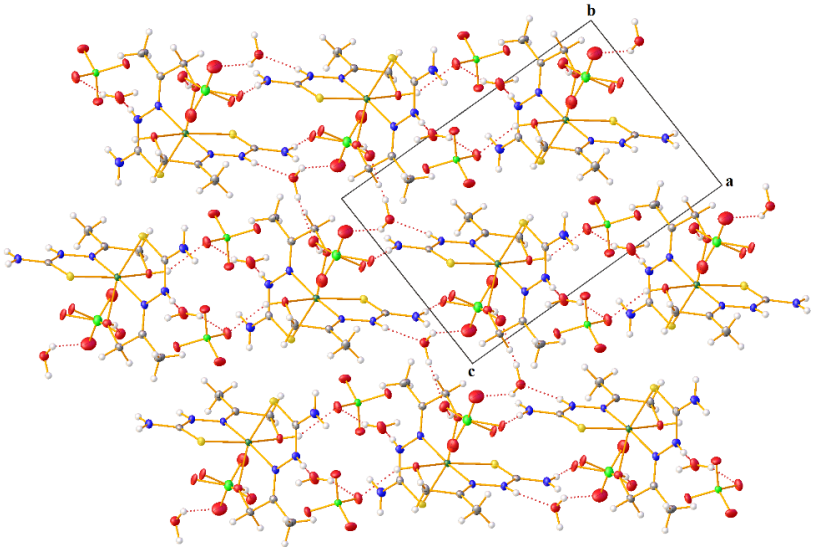

Figure 5. Packing diagram of complex **2** viewed along the *a*-axis

Intramolecular hydrogen bonds involving the OH of the coordinated alcoholic group or free water molecule as donors and oxygen atoms of free perchlorate anions as acceptors are observed (O2—H2···O6 and O12—H12A···O10). In addition, intermolecular hydrogen bonds involving the hydrazinyl NH moiety, the hydroxyl group

of the coordinated ligand or the free water molecule as donors, and oxygen atoms of free perchlorate anions as acceptor are observed (O1—H1···O10^{i}, O11—H11A···O6^{ii}, O11—H11B···O5^{iii}, N5—H5···O12^{iii}, N2—H2A···O11^{iv}) (Table 5, Fig. 5).

3.3. Crystal structure of $[Ni(H_2L)_2](NO_3)_2$ (3)

The X-ray structure determination of compound **3** derived from H_2L reveals a mononuclear dicationic compound that crystallizes in a monoclinic system with the space group *C2/c*. An ORTEP diagram of the compound formulated as $[Ni(H_2L)_2]\cdot 2(NO_3)$ is shown in Fig. 6, and the selected bond distances and angles are listed in Table 6. The asymmetric unit contains two neutral molecule ligands, one Ni^{2+} cation, and two uncoordinated nitrate anions. Each ligand acts tridentate fashion and coordinates the Ni(II) through one thione sulfur atom, one alcoholic oxygen atom, and one azomethine nitrogen atom, resulting in an $N_2O_2S_2$ core. The coordination geometry around the Ni(II) cation is best described as a distorted octahedral geometry. The basal plane is occupied by two sulfur and two oxygen atom, the apical positions being occupied by two azomethine nitrogen atoms. The sum value of the cissoid angles in the basal plane is 366.36°, while the angle subtended by the atoms in apical positions (N1—Ni1—N1^{i} = 167.52(11)°) is far from the ideal value of 180°. These observations confirm the severity of the distortion of the octahedral polyhedron. The Ni—N distances [1.9979(18) Å and 1.9980(18) Å] are in the range expected for similar compounds [37]. The Ni—S [2.3859(7) Å] and Ni—O bond lengths [2.1290(18) Å] are comparable to those reported for the analogous compound $[Ni(H_2L)_2]\cdot[(Cl)_2$ [35].

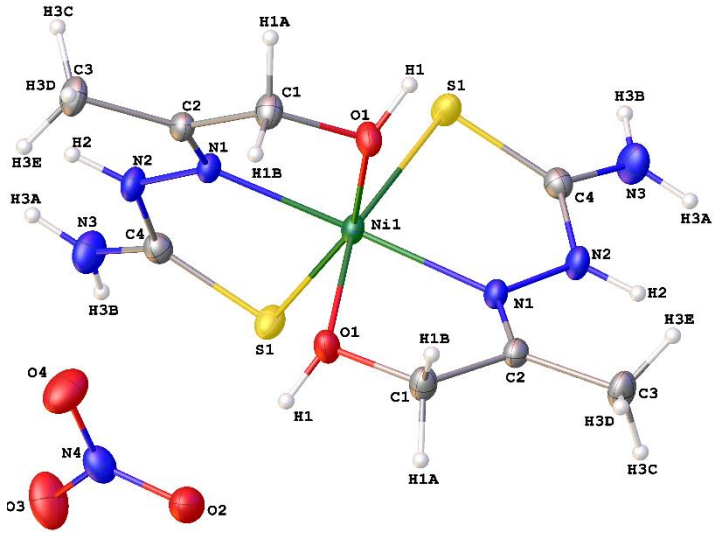

Figure 6. ORTEP view of the compound **3**

Table 6. Selected geometric parameters (Å, °).

Atoms	Distance	Atoms	Distance
Ni1—S1^{i}	2.3859 (7)	Ni1—N1	1.9979 (18)
Ni1—S1	2.3859 (7)	Ni1—N1^{i}	1.9980 (18)
Ni1—O1^{i}	2.1290 (18)	S1—C4	1.699 (3)
Ni1—O1	2.1290 (18)	O1—C1	1.426 (3)
Atoms	**Angle**	**Atoms**	**Angle**
S1^{i}—Ni1—S1	94.95 (4)	N1—Ni1—S1^{i}	105.99 (6)
O1—Ni1—S1^{i}	96.42 (5)	N1i—Ni1—S1	105.99 (6)
O1—Ni1—S1	159.14 (5)	N1—Ni1—O1	77.47 (7)
O1^{i}—Ni1—S1	96.42 (5)	N1i—Ni1—O1	92.79 (7)
O1^{i}—Ni1—S1^{i}	159.14 (5)	N1i—Ni1—O1^{i}	77.47 (7)

O1—Ni1—O1^{i}	78.57 (10)	N1—Ni1—O1^{i}	92.79 (7)
N1^{i}—Ni1—S1^{i}	82.61 (6)	N1—Ni1—N1^{i}	167.52 (11)
N1—Ni1—S1	82.61 (6)		

Symmetry code: (i) −x+1, y, −z+1/2.

Table 7. Hydrogen-bond geometry (Å, °).

D—H···*A*	*D*—H	H···*A*	*D*···*A*	*D*—H···*A*
O1—H1···O2	0.864 (9)	1.856 (10)	2.712 (3)	170.6 (19)
O1—H1···N4	0.864 (9)	2.574 (13)	3.318 (3)	144.9 (18)
N2—H2···O3^{ii}	0.86	2.39	3.046 (4)	133.2
N3—H3A···O4^{iii}	0.86	2.21	2.985 (3)	149.1
N3—H3A···O3^{iii}	0.86	2.66	3.478 (4)	159.7
N3—H3B···O4^{iv}	0.86	2.15	2.941 (3)	153.2

Symmetry codes : (ii) −x+1, −y+1, −z+1; (iii) x+1/2, y−1/2, z; (iv) −x+1, y−1, −z+1/2; (v) x, −y+1, z+1/2; (vi) −x+1, −y+2, −z+1.

In this compound, there are intramolecular hydrogen bonds involving the hydroxyl group of the coordinated ligand as a donor and the oxygen atom and the nitrogen atom of the nitrate group as a donor (O1—H1···O2 and O1—H1···N4). In addition, intramolecular hydrogen bonds involving the oxygen atoms of the nitrate group as acceptor and the hydrazinyl or the amino moieties as donor are observed (N2—H2···O3^{ii}, N3—H3A···O4^{iii}, N3—H3A···O3^{iii} and N3—H3B···O4^{iv}) (Table 7). Additionally, the structure is consolidated by hydrogen bonds involving CH as a donor [C1—H1A···S1^{v}, C3—H3C···O3^{ii} and C3—H3D···O2^{vi}] (Fig. 7).

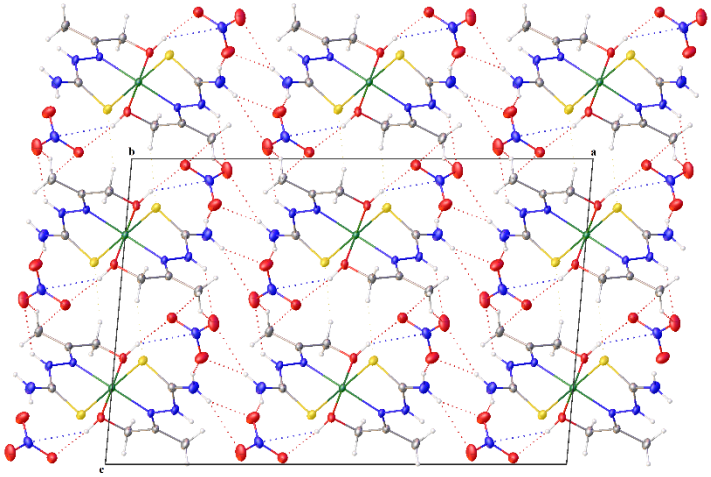

Figure 7. Packing diagram of complex **3** viewed along the *a*-axis

3.4. Crystal structure of [Ni(HL)(H$_2$L)](NO$_3$)·0.75(H$_2$O) (4)

Compound **4** crystallizes in the triclinic system with the space group Pī. The selected bond distances and angles are given in Table 8. The ORTEP representation of compound **4** is formulated as [Ni(HL)(H$_2$L)]·(NO$_3$)·0.75(H$_2$O) is shown in Fig. 8. The asymmetric unit contains one Ni(II) cation, one neutral ligand, one mono-deprotonated ligand, one nitrate anion, and 0.75 water molecule. The nickel center of the cationic moiety is coordinated with two azomethine nitrogen atoms, two alcoholic oxygen atoms, one thione sulfur atom, and one sulfide sulfur atom. The Ni—S bond lengths are different, as shown by the values of [N1—S1] 2.3523(5) Å [N1—S1] and 2.3952(5) Å [N1—S2]. Additionally, the C—S bond lengths values of 1.7321(18) Å [S1—C4] and 1.6894(18) Å [S2—C8] are different. These differences indicate the presence of thione form for one of the ligand and a thiolate form arising from

deprotonation of the hydrazinyl group for the second ligand [38,39]. The Ni—O [2.1435(14) Å, 2.1117(13) Å] and Ni—N [2.0077(14) Å, 2.0182(15) Å] bond distances are longer than those reported for similar compounds [40,41]. The Ni(II) environment is best described as octahedral geometry. The basal plane is occupied by two nitrogen atoms (N1, N4), one alcoholic oxygen atom (O2), and one thione sulfur atom (S2), the apical positions being occupied by one thiolate sulfur atom (S1) and one alcoholic oxygen atom (O1). The *cissoid* angle subtended by the atoms in the equatorial plane are in the range [76.32(5)°-106.80(4)°] while the *transoid* angles are N1—Ni1—N4 = 166.76 (6)° and O2—Ni1—S2 =158.32 (4)°. These values deviate severely from the ideal 90° and 180° values for a perfect octahedral geometry. The angle defined by the S1 and O1 atoms occupying the apical positions, 161.57(4)°, deviates severely from the ideal value of 180°. The two ligand molecules, which are quite planar (rms 0.0664 Å and 0.0497 Å), are perpendicular with a dihedral angle of 88.738(1)°. The rings NiNCCO and NiNNCS formed by each ligand are almost planar and form a dihedral angle of 3.985(1)° and 5.045(1)°, respectively, showing a slight twist in the ligand molecules. The bite angles are 83.11(4)° and 76.32(5)° for one ligand and the second ligand molecule 83.58(49)° and 78.08(6)° showing the distortion of the octahedral geometry.

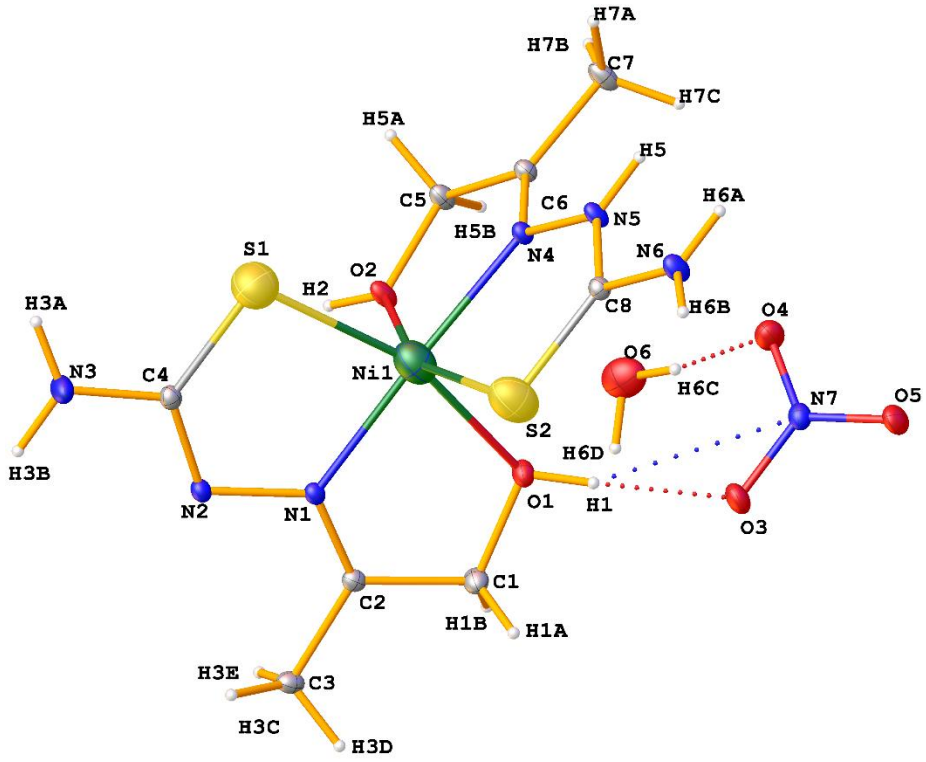

Figure 8. ORTEP view of the compound **4**

Table 8. Selected geometric parameters (Å, °).

Atoms	Distance	Atoms	Distance
Ni1—S1	2.3523 (5)	Ni1—N4	2.0182 (15)
Ni1—S2	2.3952 (5)	S1—C4	1.7321 (19)
Ni1—O2	2.1117 (13)	S2—C8	1.6894 (18)
Ni1—O1	2.1435 (14)	O2—C5	1.398 (2)
Ni1—N1	2.0077 (14)	O1—C1	1.417 (3)
Atoms	**Angle**	**Atoms**	**Angle**
S1—Ni1—S2	96.544 (19)	N1—Ni1—O2	92.61 (5)
O2—Ni1—S1	95.13 (5)	N1—Ni1—O1	78.08 (6)

O2—Ni1—S2	158.32 (4)	N1—Ni1—N4	166.76 (6)
O2—Ni1—O1	84.03 (6)	N4—Ni1—S1	104.36 (5)
O1—Ni1—S1	161.57 (4)	N4—Ni1—S2	83.11 (4)
O1—Ni1—S2	90.49 (4)	N4—Ni1—O2	76.32 (5)
N1—Ni1—S1	83.58 (4)	N4—Ni1—O1	93.35 (6)
N1—Ni1—S2	106.80 (4)		

Table 9. Hydrogen-bond geometry (Å, °).

D—H···*A*	*D*—H	H···*A*	*D*···*A*	*D*—H···*A*
O2—H2···N2^{i}	0.851 (9)	1.845 (10)	2.6790 (19)	166 (2)
O1—H1···O3	0.863 (9)	1.880 (11)	2.732 (2)	169 (2)
O1—H1···N7	0.863 (9)	2.658 (11)	3.459 (2)	155.0 (16)
N5—H5···O5^{ii}	0.86	2.05	2.902 (2)	170.2
N6—H6A···O4^{ii}	0.86	2.21	3.034 (3)	161.1
N6—H6B···S1^{iii}	0.86	2.68	3.4799 (17)	156.1
N3—H3A···O5^{iv}	0.90	2.22	3.098 (3)	164.7
N3—H3B···O6^{v}	0.92	2.36	3.081 (4)	135.3
O6—H6C···O4	0.85	2.36	3.182 (4)	162.7
O6—H6D···O3^{vi}	0.85	2.31	3.135 (4)	164.9

Symmetry codes: (i) −x, −y+1, −z+1; (ii) −x+1, −y, −z; (iii) −x+1, −y+1, −z; (iv) x−1, y+1, z; (v) x, y+1, z; (vi) −x+1, −y, −z+1; (vii) x−1, y, z.

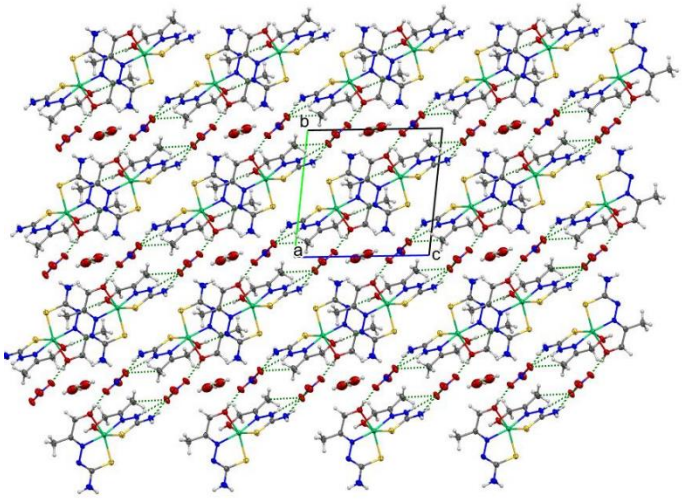

Figure 9. Packing diagram of complex **4** viewed along the *a*-axis

Intramolecular hydrogen bonds of type O_{water}—H···O_{NO_3} (O6—H6C···O4), $O_{alcoholic}$—H···O_{NO_3} (O1—H1···O3), and $O_{alcoholic}$—H···N_{NO_3} (O1—H1···N7) connect the cationic moiety, the free water molecule, and the anionic moiety in the asymmetric unit. Numerous intermolecular hydrogen of type $O_{alcoholic}$—H···N_{imino} (O2—H2···N2^{i}; i = −x, −y+1, −z+1); $N_{hydrazinyl}$—H···O_{NO_3} (N5—H5···O5^{ii}; ii = −x+1, −y, −z); Namino—H···O_{NO_3} (N6—H6A···O4^{ii};

N3—H3A···O5^{iv}; iv = x−1, y+1, z; N3—H3B···O6^{v}; v = x, y+1, z), $N_{hydrazinyl}$—H···S (N6—H6B···S1^{iii}; iii = −x+1, −y+1, −z) and O_{water}—H···O_{NO_3} (O6—H6D···O3^{vi}; vi = −x+1, −y, −z+1). Weak intermolecular hydrogen bonds involving $C_{Methylene}$—H···$S_{thiolate}$(C3—H3E···S1^{i}); $C_{Methylene}$—H···S_{thione} (C7-H7A···S2^{i}) and (C5—H5A···S2^{vii}; vii = -x−1, y, z), C_{Methyl}—H···O_{NO_3} (C7—H7A···O5^{ii});$C_{Methylene}$—H···N_{NO_3} (C1— H1B···N7^{vi}). The combined hydrogen bond links create a three-dimensional network (Table 9, Fig. 9).

3.5. Crystal structure of [Cu(H$_2$L)Cl](Cl)·0.5H$_2$O (5)

The compound (**5**) crystallizes in the monoclinic system, and the molecular structure was satisfactorily calculated in *C2/c* space group. The selected bond distances and angles are listed in Table 10, and the ORTEP view of the compound formulated as [Cu(H$_2$L)Cl](Cl)·0.5H$_2$O is illustrated in Fig. 10. The asymmetric unit contains one copper (II) ion one non-deprotonated ligand, one coordinated chloride anion, one uncoordinated chloride anion, and a one-half uncoordinated water molecule. The compound is built as mononuclear, and the Cu(II) cation is coordinated to the ligand through one azomethine nitrogen atom, one alcoholic oxygen atom, and one thione sulfur atom. One chloride anion completes the coordination sphere yielding a NOSCl chromophore. The environment of the tetracoordinate copper (II) is best described as a square planar geometry as shown by the tetragonality parameter τ_4 of 0.2205 (τ_4 = (360 – α – β) / 141: α and β are the two largest angles around the central atom; t_4 = 0 designates a perfect square planar geometry and t_4 = 1 gives a perfect tetrahedron) [42]. In fact, the bond angle values of 99.49(3)° [Cl1—Cu1—S1], 77.90(7)° [N3—Cu1—O1], 85.80(5)° [N3—Cu1—S1], 95.19(6)° [O1—Cu1—Cl1] are severely deviated from the ideal value of 90° for a perfect square planar geometry. The sum of the angles subtended by the atoms in the plane is 358.32°. The distance C1—S1 of 1.715 (2) Å, consistent with a double bond character [43], indicates the presence of the thione moiety in the coordinated ligand. The Cu1—O1 [1.9918(18 Å], Cu1—N3 [1.9601(17) Å], Cu1—Cl1 [2.2063(6) Å], and Cu1—S1 [2.2648(7) Å] are comparable to the corresponding values found for the copper compound with the same ligand in which, the copper(II) cation is pentacoordinate [44].

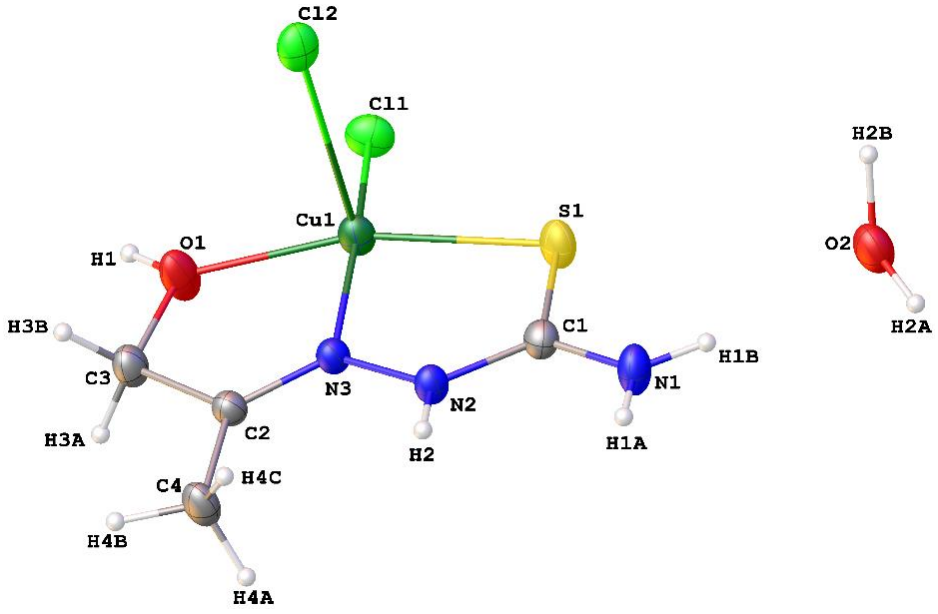

Figure 10. ORTEP view of the compound **5**

Table 10. Selected geometric parameters (Å, °).

Atoms	Distance	Atoms	Distance
Cu1—N3	1.9601 (17)	Cu1—S1	2.2648 (7)
Cu1—O1	1.9918 (18)	S1—C1	1.715 (2)
Cu1—Cl1	2.2063 (6)	O1—C3	1.414 (3)
Atoms	**Angle**	**Atoms**	**Angle**
N3—Cu1—O1	77.90 (7)	N3—Cu1—S1	85.80 (5)

N3—Cu1—Cl1	166.17 (6)	O1—Cu1—S1	162.74 (6)
O1—Cu1—Cl1	95.19 (6)	Cl1—Cu1—S1	99.49 (3)

Table 11. Hydrogen-bond geometry (Å, °).

D—H···*A*	*D*—H	H···*A*	*D*···*A*	*D*—H···*A*
O1—H1···Cl2^{i}	0.843 (9)	2.133 (9)	2.9699(18)	171.7 (19)
N2—H2···Cl2^{ii}	0.86	2.30	3.1291 (18)	161.5
N1—H1A···Cl2^{ii}	0.86	2.66	3.410(2)	146.7
N1—H1B···O2	0.86	2.10	2.936 (7)	163.8
N1—H1B···O2^{iii}	0.86	2.05	2.899 (7)	170.7
O2—H2A···Cl1^{v}	0.99	2.87	3.423 (5)	116.4
O2—H2A···Cl1^{vi}	0.99	2.64	3.425 (5)	136.6
O2—H2B···Cl2^{vii}	1.12	2.13	3.241 (4)	170.7

Symmetry codes : (i) −*x*+3/2, −*y*+3/2, −*z*+1; (ii) −*x*+3/2, −*y*+1/2, −*z*+1; (iii) −*x*+1, *y*, −*z*+1/2; (iv) *x*, −*y*+1, *z*+1/2; (v) −*x*+1, *y*−1, −*z*+1/2; (vi) *x*, *y*−1, *z*; (vii) −*x*+3/2, *y*−1/2, −*z*+1/2.

The hydrogen bonding geometry of the compound is listed in Table 11. Intramolecular hydrogen bond N_{amino}—H···O_{water} (N1—H1B···O2) links the free water molecule to the compound molecule. Numerous intermolecular hydron bonds of type N—H···Cl (N2—H2···Cl2^{ii}, ii = −*x*+3/2, −*y*+1/2, −*z*+1), O—H···Cl (O2—H2A···Cl1^{v}, v = −*x*+1, *y*−1; O2—H2A···Cl1^{vi}, vi = *x*, *y*−1, *z*; O1—H1···Cl2^{i}, i = −*x*+3/2, −*y*+3/2, −*z*+1), and C—H···Cl (C3—H3B···Cl1^{i}, i = −*x*+3/2, −*y*+3/2, −*z*+1; C4—H4B···Cl2^{iv} and- C4—H4B···Cl2^{iv}, iv = *x*, −*y*+1, *z*+1/2) (Table 11) links the molecules yielding several chains superimposed on each other. The chain is linked by O—H···Cl (O2—H2B···Cl2^{vii} vii = −*x*+3/2, *y*−1/2, −*z*+1/2) and N—H···O (N1—H1B···O2^{iii}; iii = −*x*+1, *y*, −*z*+1/2) (Table 11) bonds which ensure the cohesion and stability of the structure as shown in Fig. 11.

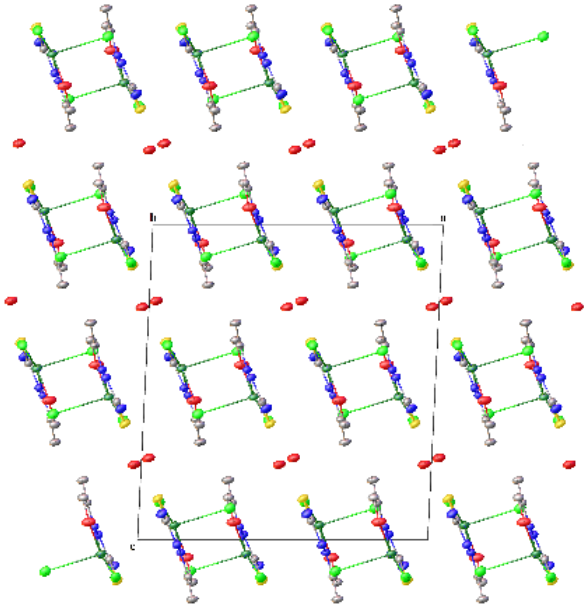

Figure 11. Packing diagram of complex **5** viewed along the *a*-axis

3.6. Crystal structure of $[Zn(H_2L)_2](ClO_4)_2{\cdot}2H_2O$ (6)

The hexacoordinated zinc(II) compound **6** crystallizes in the monoclinic system with the space group *C2/c*. The selected bond distances and angles are listed in Table 12**,** and the *ORTEP* representation of **6** is shown in Fig. 12. The asymmetric unit of the crystal structure of compound **6** contains one $[Zn(H_2L)_2]^{2+}$, two uncoordinated perchlorate anions ClO_4^{-}, and two free water molecules. The two ligand molecules act tridentate through the azomethine nitrogen atom, the sulfur atom, and the alcoholic oxygen atom.

Thus, the Zn^{2+} cation is situated in an $N_2O_2S_2$ inner, and its coordination sphere is best described as a distorted octahedral polyhedron. The sulfur and the oxygen atoms occupy the equatorial plane, while the imino nitrogen atoms occupy the axial positions. The *transoid* angles in are in the range [150.18(15)°—155.37(7)°] while the *cissoid* angles are in the range [71.90(10)°—116.21(7)°]. These values deviate severely from the ideal values of 180 and 90° for a perfect octahedral environment. The two tridentate ligand molecules are quite planar (rms 0.0912), with the sulfur atom 0.1756(1) Å out of the plane. The two mean planes of the ligand molecules form a dihedral angle of 83.70°. Each ligand forms two five membered-ring of type Zn1S1C4N2N1 and Zn1N1C2C1O1 with bite angles of S1—Zn1—N1 = 83.47 (7)° and N1—Zn1—O1 = 71.90 (10)°. The two five-membered rings are twisted at 6.660(2)° dihedral angles. The two ligand molecules act in their thione and alcoholic forms as indicated by the distances C4=S1 [1.694 (4)Å] and C1—O1 [1.401 (5) Å]. The bond distances Zn1—S 2.3971(9) [Å], Zn1—N [2.088(2) Å], and Zn1—O [2.327(3) Å] are by the values reported for similar complexes [45–47]. The free perchlorate anions are constrained to be tetrahedral, as shown by the angle values O—Cl—O (Table 2). The mononuclear unit and the perchlorate anion of the asymmetric unit are connected by intramolecular hydrogen bonds of type N_{amino}–H…$OClO_3$ (N3–H3B…O5), N_{amino}–H…O_{water} (N3–H3B…O2) and $N_{hydrazinyl}$–H…O_{water} (N2—H2···O2) (Fig. 13, Table 13). Intermolecular hydrogen bond of type $O_{alcoholic}$–H…ClO_4 (O1—H1···Cl1^{ii}; ii = x+1/2, −y+1/2, z+1/2) and $O_{alcoholic}$–H…$OClO_3$ (O1—H1···O3^{ii}) and weak intermolecular hydrogen bonds involving C–H…$OClO_3$ (C1—H1B···O4^{iii} ; iii = −x+3/2, −y+1/2, −z+1) and C_{imino}–H…$O_{phenoxo}$ (C27—H27···O5^{iii} ; iii =−x+1, −y+1, −z) and C_{imino}–H…$OClO_3$ (C34—H34···O9^{ii}; ii = −x+1, −y+1, −z+1) link the mononuclear units belonging to different asymmetric units. The combined hydrogen bond links give rise to a three-dimensional network architecture. It should be noted that the perchlorate ion is engaged in numerous interactions in the structure.

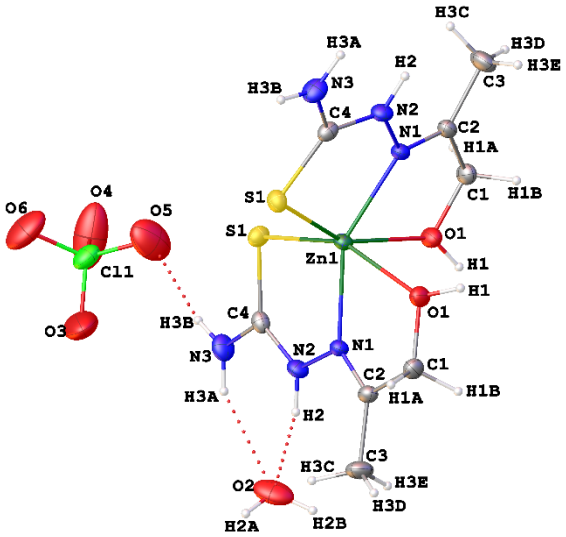

Figure 12. ORTEP view of the compound **6**

Table 12. Selected geometric parameters (Å, °).

Atoms	Distance	Atoms	Distance
Zn1—N1^{i}	2.088 (2)	Zn1—S1^{i}	2.3971 (9)
Zn1—N1	2.088 (2)	Zn1—S1	2.3971 (9)
Zn1—O1	2.327 (3)	S1—C4	1.694 (4)
Zn1—O1^{i}	2.327 (3)	O1—C1	1.401 (5)
Atoms	**Angle**	**Atoms**	**Angle**
N1i—Zn1—N1	150.18 (15)	N1—Zn1—S1	83.47 (7)
N1i—Zn1—O1	86.66 (10)	O1—Zn1—S1	155.37 (7)
N1—Zn1—O1	71.90 (10)	O1i—Zn1—S1	90.25 (8)

N1i—Zn1—O1^{i}	71.90 (10)	S1i—Zn1—S1	100.85 (5)
N1—Zn1—O1^{i}	86.66 (10)	O3—Cl1—O6	109.3 (5)
O1—Zn1—O1^{i}	88.40 (15)	O3—Cl1—O5	109.3 (6)
N1i—Zn1—S1^{i}	83.47 (7)	O6—Cl1—O5	122.6 (6)
N1—Zn1—S1^{i}	116.21 (7)	O3—Cl1—O4	103.6 (10)
O1—Zn1—S1^{i}	90.26 (8)	O6—Cl1—O4	105.8 (5)
O1i—Zn1—S1^{i}	155.37 (7)	O5—Cl1—O4	104.4 (6)
N1i—Zn1—S1	116.21 (7)		

Symmetry code: (i) −x+2, y, −z+3/2.

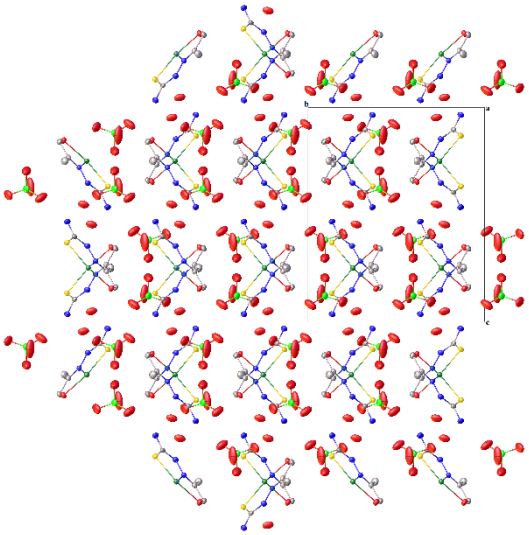

Figure 13. Packing diagram of complex **2** viewed along the *a*-axis

Table 13. Hydrogen-bond geometry (Å, °).

D—H···A	D—H	H···A	D···A	D—H···A
O1—H1···Cl1^{ii}	0.854 (9)	2.914 (18)	3.701 (3)	154 (3)
O1—H1···O3^{ii}	0.854 (9)	1.89 (2)	2.705 (7)	159 (5)
N2—H2···O2	0.86	2.01	2.810 (5)	155.2
N3—H3A···O2	0.86	2.22	2.976 (7)	145.9
N3—H3B···O5	0.86	2.21	3.062 (9)	170.3

Symmetry codes : (ii) x+1/2, −y+1/2, z+1/2; (iii) −x+3/2, −y+1/2, −z+1.

3.7. General study

The H_2L ligand was characterized by spectroscopic methods such as FTIR and ^{1}H and ^{13}C NMR. The FTIR spectrum (Fig. 14) of the ligand H_2L gives several characteristic bands. The broad band at 3380 cm^{-1} indicates the presence of a hydroxy group in the molecule. The bands at 3217 and 3164 cm^{-1} are attributed to the -NH_2 amino group. The band at 3139 cm^{-1} is due to the stretching of the N-H bond of the hydrazinyl group. The CH vibration modes due to -CH_2- and -CH_3 groups are pointed as weak intensity bands between 3031 and 2849 cm^{-1} [48]. The band due to the C=N moiety is pointed at 1603 cm$^{-1,}$ while the characteristic bands due to the thioamide NH-C=S moieties are pointed at 1259 and 791 cm^{-1}. The absence of the band characteristic of the S-H, expected at *ca.* 2600 cm^{-1}, indicates that the compound is only in its thione form. The ligand's 1H NMR spectrum (Fig. 15) shows a broad signal characteristic of the OH group at 4.88 ppm. Two singlet

signals at 4.01 and 1.87 ppm are also observed, attributed to the -CH_2- and -CH_3 groups, respectively. The signals at 7.90 and 8.06 ppm are attributed to the two protons of the -NH_2 group. The signal at δ 10.01 ppm is due to the -NH proton. The ^{13}C NMR spectrum (Fig. 16) of the ligand shows signals at 153.08 ppm and 179.54 ppm attributed to azomethine (C=N) and thiocarbonyl (C=S) carbon atoms, respectively.

Upon coordination of H_2L to metal the ions, the band due to the C=N stretching, which appears at 1603 cm^{-1} in the ligand spectrum, is shifted to low frequencies for all the compounds [1592 cm^{-1} -1639 cm^{-1}]. The band due to C=S stretching is shifted from 1259 cm^{-1} (in H_2L) to 1252-1228 cm^{-1} (in the complexes). The ν_{OH} pointed at 3380 cm^{-1} in the spectrum of the ligand is shifted to low frequencies. These observations indicate the involvement of the azomethine nitrogen atom, the sulfur thione atom, and the alcoholic oxygen atom in coordinating with the relative metal ion [49]. The spectra of compounds (**1**), (**3**), and (**4**) show a sharp and strong band at *ca*. 1380 cm^{-1} attributed to the nitrate ion [50]. The IR spectrum of compound (**2**) presents additional bands at 620 cm^{-1} and 1070 cm^{-1} due to the presence of perchlorate anion [51].

The electronic absorption spectral analysis of the six metal complexes exhibits absorption bands at 225 nm and 298 nm due to π→π* electronic transition in the azomethine chromophore. The compounds also exhibit a band at *ca*. 405 nm due to n→π* electronic transition in the azomethine chromophore. High-spin cobalt(II) octahedral complex, allows three spin permissible d→d transitions, namely $^4T_{1g}(F)\rightarrow{}^4T_{2g}(F)$, $^4T_{1g}(F)\rightarrow{}^2A_{2g}$ and $^4T_{1g}(F)\rightarrow{}^4T_{1g}(P)$ [52]. With compound (**1**), these first bands appear over the near-IR range at 1080 nm. In the visible range of the spectrum, only one asymmetric band appears at 532 nm. The magnetic moment value of 5.9 μ_B indicates a mononuclear compound in which the high-spin Co(II) cation is in an octahedral environment [53]. For compounds **2**, **3,** and **4** two bands in the ranges of 522-544 nm and 780-880 nm are dues to the allowed $^3A_2(^3F)\rightarrow{}^3T_1(^3F)$ and $^3A_2(^3F)\rightarrow{}^3T_1(^3P)$ transitions for octahedral geometry [50]. The magnetic moment of values 3.37 μ_B for **2**, 3.46 μ_B for **3,** and 3.49 μ_B for **4** indicate a mononuclear compound for d^8 Ni(II) with octahedral geometry [51]. Compound (**6**) is paramagnetic. For the copper(II) compound (**5**) a low energy band at 591 nm attributed to d→d transition indicating a square-planar geometry around the Cu(II) cation. These facts are characteristic of a distorted square-planar environment [54]. The magnetic moment value of 1.69 μ_B for compound (**5**) is near that of 1.72 μ_B reported for a mononuclear square-planar copper(II) compound [55]. The molar conductivity values, which are in the range 130-170 $S{\cdot}cm^2{\cdot}mol^{-1}$ for compounds (**1**), (**2**), (**3**), and (**6**) show that compounds are 2:1 electrolytes in DMF solution [56]. Compounds (**4**) and (**5**) are 1:1 electrolytes, as shown by their conductivity values of 65.7 and 75 $S{\cdot}cm^2{\cdot}mol^{-1}$, respectively. All the compounds are stable in the DMF solution owing to the slow conductivities increase two weeks later.

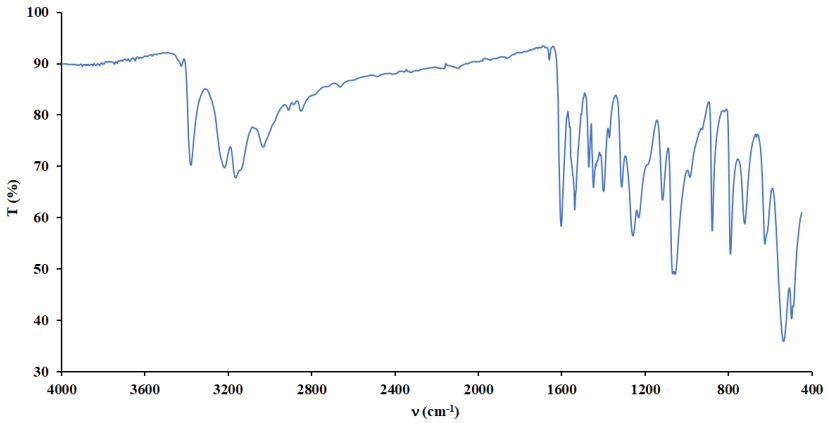

Figure 14. FTIR spectrum of H_2L

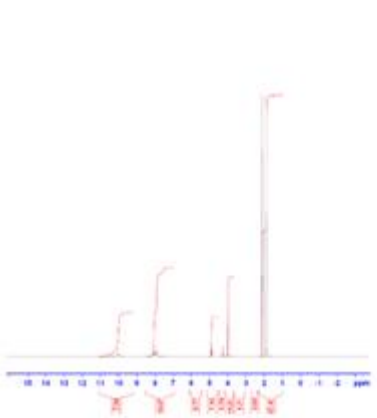

Figure 15. ^{1}H NMR spectrum of H_2L

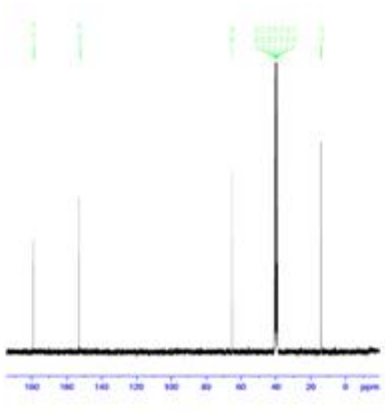

Figure 16. ^{13}C NMR spectrum of H_2L

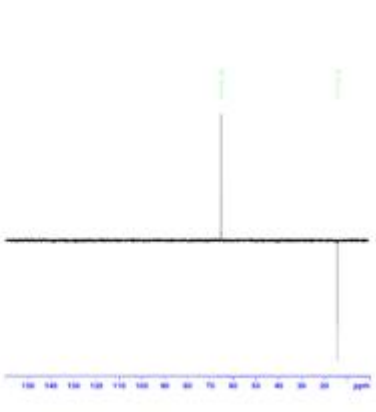

Figure 17. DEPT 135 ^{13}C NMR spectrum of H_2L

4. Conclusion

The H_2L ligand with the thiosemicarbazide moiety showed similar mode coordination through the six compounds' O, N, and S donor atoms. All the structures of the six compounds are established by single X-ray diffraction. The coordination compounds $[Co(H_2L)_2](NO_3)_2$, $[Ni(H_2L)_2](ClO_4)_2{\cdot}2H_2O$, $[Ni(H_2L)_2]$ $(NO_3)_2$ and $[Zn(H_2L)_2](ClO_4)_2{\cdot}2H_2O$ are 2:1 electrolytes in DMF solutions. In compound $[Ni(HL)(H_2L)]$ $(NO_3){\cdot}0.75(H_2O)$, one of the ligand molecules acts in its mono-deprotonated form. At the same time, the second reacts in its non-deprotonated form yielding a 1:1 electrolyte compound in DMF solution. In compound $[Cu(H_2L)Cl](Cl){\cdot}0.5H_2O$, only one non-deprotonated ligand molecule is involved in the coordination yielding and 1:1 electrolyte in DFM solution. On considering the magnetic moments of the compounds, it appears that compounds $[Co(H_2L)_2](NO_3)_2$, $[Ni(H_2L)_2](ClO_4)_2{\cdot}2H_2O$,$[Ni(H_2L)_2](NO_3)_2$, $[Ni(HL)(H_2L)](NO_3){\cdot}0.75(H_2O)$, $[Cu(H_2L)Cl](Cl){\cdot}0.5H_2O$ are mononuclear. Compound $[Zn(H_2L)_2](ClO_4)_2{\cdot}2H_2O$ is diamagnetic in nature. The structures of the compounds are consolidated by classical H-bond involving the $-NH_2$, NH and/or OH groups.

References

1- O.A. El-Gammal, G.M.A. El-Reash, M.M. El-Gamil, Structural, spectral, pH-metric and biological studies on mercury (II), cadmium (II) and binuclear zinc (II) complexes of NS donor thiosemicarbazide ligand, Spectrochim. Acta, Part A, **2014**, 123, 59–70. https://doi.org/10.1016/j.saa.2013.12.034.

2- A. Basu, G. Das, Zn(II) and Hg(II) complexes of naphthalene based thiosemicarbazone: Structure and spectroscopic studies, Inorg. Chim. Acta, **2011**, 372(1), 394–399. https://doi.org/10.1016/j.ica.2011.01.097.

3- B. Wang, Z.-Y. Yang, M. Lü, J. Hai, Q. Wang, Z.-N. Chen, Synthesis, characterization, cytotoxic activity and DNA binding Ni(II) complex with the 6-hydroxy chromone-3-carbaldehyde thiosemicarbazone, J. Organomet. Chem., **2009**, 694(25), 4069–4075. https://doi.org/10.1016/j.jorganchem.2009.08.024.

4- H. Hosseinpoor, S.M. Farid, A. Iraji, M.S. Asgari, N. Edraki, S. Hosseini, A. Jamshidzadeh, B. Larijani, M. Attarroshan, S. Pirhadi, M. Mahdavi, M. Khoshneviszadeh, Anti-melanogenesis and anti-tyrosinase properties of aryl-substituted acetamides of phenoxy methyl triazole conjugated with thiosemicarbazide: Design, synthesis, and biological evaluations, Bioorg. Chem., **2021**, 114, 104979. https://doi.org/10.1016/j.bioorg.2021.104979.

5- F.S. Tokalı, P. Taslimi, H. Usanmaz, M. Karaman, K. Şendil, Synthesis, characterization, biological activity, and molecular docking studies of novel Schiff bases derived from thiosemicarbazide: Biochemical and computational approach, J. Mol. Struct., **2021**, 1231, 129666. https://doi.org/10.1016/j.molstruc.2020.129666.

6- Z. Bakherad, M. Mohammadi-Khanaposhtani, H. Sadeghi-Aliabadi, S. Rezaei, A. Fassihi, M. Bakherad, H. Rastegar, M. Biglar, L. Saghaie, B. Larijani, M. Mahdavi, New thiosemicarbazide-1,2,3-triazole hybrids as potent α-glucosidase inhibitors: Design, synthesis, and biological evaluation, J. Mol. Struct., **2019**, 1192, 192–200. https://doi.org/10.1016/j.molstruc.2019.04.082.

7- H.A. Aboseada, M.M. Hassanien, I.H. El-Sayed, E.A. Saad, Schiff base 4-ethyl-1-(pyridin-2-yl) thiosemicarbazide up-regulates the antioxidant status and inhibits the progression of Ehrlich solid tumor in mice, Biochem. Biophys. Res. Commun., **2021**, 573, 42–47. https://doi.org/10.1016/j.bbrc.2021.07.102.

8- A.A. Altalhi, H.E. Hashem, N.A. Negm, E.A. Mohamed, E.M. Azmy, Synthesis, characterization, computational study, and screening of novel 1-phenyl-4-(2-phenylacetyl)-thiosemicarbazide derivatives for their antioxidant and antimicrobial activities. J. Mol. Liq., **2021**, 333, 115977. https://doi.org/10.1016/j.molliq.2021.115977.

9- L.S. Munaretto, M. Ferreira, D.P. Gouvêa, A.J. Bortoluzzi, L.S. Assunção, J. Inaba, T.B. Creczynski-Pasa, M.M. Sá, Synthesis of isothiosemicarbazones of potential antitumoral activity through a multicomponent reaction involving allylic bromides, carbonyl compounds and thiosemicarbazide, Tetrahedron, **2020**, 76(23), 131231. https://doi.org/10.1016/j.tet.2020.131231.

10- D.B. Patel, D.G. Darji, K.R. Patel, D.P. Rajani, S.D. Rajani, H.D. Patel, Synthesis of novel quinoline-thiosemicarbazide hybrids and evaluation of their biological activities, molecular docking, molecular dynamics, pharmacophore model studies, and ADME-Tox properties, J. Heterocycl. Chem., **2020**, 57(3), 1183–1200. https://doi.org/10.1002/jhet.3855.

11- D.B. Patel, K.D. Patel, N.P. Prajapati, K.R. Patel, D.P. Rajani, S.D. Rajani, N.S. Shah, D.D. Zala, H.D. Patel, Design, Synthesis, and Biological and In Silico Study of Fluorine-Containing Quinoline Hybrid Thiosemicarbazide Analogues, J. Heterocycl. Chem., **2019**, 56(8), 2235–2252. https://doi.org/10.1002/jhet.3617.

12- B. Šarkanj, M. Molnar, M. Čačić, L. Gille, 4-Methyl-7-hydroxycoumarin antifungal and antioxidant activity enhancement by substitution with thiosemicarbazide and thiazolidinone moieties, Food Chem., **2013**, 139(1), 488–495. https://doi.org/10.1016/j.foodchem.2013.01.027.

13- T. Panneerselvam, J.R. Mandhadi, Microwave assisted synthesis and antimicrobial evaluation of novel substituted thiosemicarbazide derivatives of pyrimidine, J. Heterocycl. Chem., **2020**, 57(8), 3082–3088. https://doi.org/10.1002/jhet.4013.

14- P.T. Acharya, Z.A. Bhavsar, D.J. Jethava, D.B. Patel, H.D. Patel, A review on development of bio-active thiosemicarbazide derivatives: Recent advances, J. Mol. Struct., **2021**, 1226, 129268. https://doi.org/10.1016/j.molstruc.2020.129268.

15- M.S. Refat, A.A.M. Belal, I.I. El-Deen, N. Hassan, R. Zakaria, Synthesis, spectroscopic, thermal, and antimicrobial investigations of new mono and binuclear Cu(II), Co(II), Ni(II), and Zn(II)

thiosemicarbazide complexes, J. Mol. Struct., **2020**, 1218(5), 128516. https://doi.org/10.1016/j.molstruc.2020.128516.
16- Y. Wang, H.-Q. Chang, W.-N. Wu, X.-J. Mao, X.-L. Zhao, Y. Yang, Z.-Q. Xu, Z.-H. Xu, L. Jia, A highly sensitive and selective colorimetric and off–on fluorescent chemosensor for Cu^{2+} based on rhodamine 6G hydrazide bearing thiosemicarbazide moiety, J. Photochem. Photobiol. A Chem., **2017**, 335, 10-16. https://doi.org/10.1016/j.jphotochem.2016.11.003.
17- V. Arion, K. Wieghardt, T. Weyhermueller, E. Bill, V. Leovac, A. Rufinska, Synthesis, structure, magnetism, and spectroscopic properties of some mono- and dinuclear nickel complexes containing noninnocent pentane-2,4-dione bis(*S*-alkylisothiosemicarbazonate)- derived ligands, Inorg. Chem., **1997**, 36, 661–669. https://doi.org/10.1021/ic960802o.
18- A. Fetoh, M.A. Mohammed, M.M, Youssef, G.M.A. El-Reash, Investigation (IR, UV-visible, fluorescence, X-ray diffraction and thermogravimetric) studies of Mn(II), Fe(III) and Cr(III) complexes of thiosemicarbazone derived from 4-pyridyl thiosemicarbazide and monosodium 5-sulfonatosalicylaldehyde and evaluation of their biological applications, J. Mol. Struct., **2023**,1271, 134139. https://doi.org/10.1016/j.molstruc.2022.134139.
19- N. Raman, A. Selvan, P. Manisankar, Spectral, magnetic, biocidal screening, DNA binding and photocleavage studies of mononuclear Cu(II) and Zn(II) metal complexes of tricoordinate heterocyclic Schiff base ligands of pyrazolone and semicarbazide/thiosemicarbazide based derivatives, Spectrochim. Acta, Part A, **2010**, 76(2), 161–173. https://doi.org/10.1016/j.saa.2010.03.007.
20- S. Chandra, X. Sangeetika, EPR, magnetic and spectral studies of copper(II) and nickel(II) complexes of Schiff base macrocyclic ligand derived from thiosemicarbazide and glyoxal. Spectrochim, Acta, Part A, 60(1), **2004**, 147–153. https://doi.org/10.1016/S1386-1425(03)00220-8.
21- A. Shaikh, P. Mukherjee, S. Ta, A. Bhattacharyya, A. Ghosh, D. Das, Oxidative cyclization of thiosemicarbazide: a chemo dosimetric approach for the highly selective fluorescence detection of cerium(IV), New J. Chem., **2020**, 44(22), 9452–9455. https://doi.org/10.1039/D0NJ01100B.
22- Y. Wang, H.-Q. Chang, W.-N. Wu, X.-J. Mao, X.-L. Zhao, Y. Yang, Z.-Q. Xu, Z.-H. Xu, L. Jia, A highly sensitive and selective colorimetric and off–on fluorescent chemosensor for Cu^{2+} based on rhodamine 6G hydrazide bearing thiosemicarbazide moiety, J. Photochem. Photobiol., A, **2017**, 335, 10–16. https://doi.org/10.1016/j.jphotochem.2016.11.003.
23- S. Angupillai, J.-Y. Hwang, J.-Y. Lee, B.A. Rao, Y.-A. Son, Efficient rhodamine-thiosemicarbazide-based colorimetric/fluorescent 'turn-on' chemo dosimeters for the detection of Hg^{2+} in aqueous samples, Sens. Actuators, B, **2015**, 214, 101–110. https://doi.org/10.1016/j.snb.2015.02.126.
24- M. Salavati-Niasari, Host (nanocage of zeolite–Y)/guest manganese(II), cobalt(II), nickel(II) and copper(II) complexes of 12-membered macrocyclic Schiff-base ligand derived from thiosemicarbazide and glyoxal) nanocomposite materials: Synthesis, characterization and catalytic oxidation of cyclohexene, J. Mol. Catal. A: Chem., **2008**, 283(1), 120–128. https://doi.org/10.1016/j.molcata.2007.12.015.
25- B. Pouramiri, E.T. Kermani, Lanthanum(III) chloride/chloroacetic acid as an efficient and reusable catalytic system for the synthesis of new 1-((2-hydroxynaphthalen-1-yl) (phenyl) methyl) semicarbazides/thiosemicarbazides, Arabian J. Chem., **2017**, 10, S730–S734. https://doi.org/10.1016/j.arabjc.2012.11.016.
26- M.R. Maurya, B. Sarkar, A. Kumar, N. Ribeiro, A. Miliute, J.C. Pessoa, New thiosemicarbazide and dithiocarbazate based oxidovanadium(IV) and dioxidovanadium(V) complexes. Reactivity and catalytic potential, New J. Chem., **2019**, 43(45), 17620–17635. https://doi.org/10.1039/C9NJ01486A.
27- P.P. Netalkar, S.P. Netalkar, V.K. Revankar, Transition metal complexes of thiosemicarbazone: Synthesis, structures and invitro antimicrobial studies, Polyhedron, **2015**, 100, 215–222. https://doi.org/10.1016/j.poly.2015.07.075.
28- O.V. Dolomanov, L.J. Bourhis, R.J. Gildea, J.A.K. Howard, H. Puschmann, OLEX2: a complete structure solution, refinement and analysis program, J. Appl. Crystallogr., **2009**, 42(2), 339–341. https://doi.org/10.1107/S0021889808042726.
29- G.M. Sheldrick, SHELXT – Integrated space-group and crystal-structure determination, Acta Crystallogr., Sect. A: Found. Adv., **2015**, C71, 3–8. https://doi.org/10.1107/S2053273314026370.
30- G.M. Sheldrick, Crystal structure refinement with SHELXL, Acta Crystallogr., Sect. C: Struct. Chem., **2015**, 71(1), 3–8. https://doi.org/10.1107/S2053229614024218.
31- L.J. Farrugia, WinGX and ORTEP for Windows: an update, J. Appl. Crystallogr., **2012**, 45(4), 849–854. https://doi.org/10.1107/S0021889812029111.
32- J. García-Tojal, A. García-Orad, A.A. Díaz, J.L. Serra, M.K. Urtiaga, M.I. Arriortua, T. Rojo, Biological activity of complexes derived from pyridine-2-carbaldehyde thiosemicarbazone: Structure of $[Co(C_7H_7N_4S)_2][NCS]$, J. Inorg. Biochem., **2001**, 84(3), 271–278. https://doi.org/10.1016/S0162-0134(01)00184-2.
33- X. Fan, J. Dong, R. Min, Y. Chen, X. Yi, J. Zhou, S. Zhang, Cobalt(II) complexes with thiosemicarbazone as potential antitumor agents: synthesis, crystal structures, DNA interactions, and cytotoxicity, J. Coord. Chem., **2013**, 66(24), 4268–4279. https://doi.org/10.1080/00958972.2013.867030.
34- A. Baysal, M. Aydemir, F. Durap, S. Özkar, L.T. Yildirim, Synthesis and structural characterization of a novel seven-coordinate cobalt(II) complex: 2,9-Bis (ethanolamine)-1,10-phenanthrolinechlorocobalt(II)

chloride, Inorg. Chim. Acta, **2011**, 371(1), 107–110. https://doi.org/10.1016/j.ica.2011.03.050.
35- P.P. Netalkar, S.P., Revankar, V.K. Netalkar, Transition metal complexes of thiosemicarbazone: Synthesis, structures and invitro antimicrobial studies, Polyhedron, **2015**, 100, 215–222. https://doi.org/10.1016/j.poly.2015.07.075.
36- A.V. Pestov, P.A. Slepukhin, O.V. Koryakova, V.N. Charushin, Nickel(II) and copper(II) complexes based on N-(2-carboxyethyl)alkanolamines: Influence of the amino alcohol structure on the coordination sphere of the metal center, Russian J. Coord. Chem., **2014**, 40(4), 216–223. https://doi.org/10.1134/S107032841404006X.
37- A.A. El-Sherif, A. Fetoh, Y.K. Abdulhamed, G.M.A. El-Reash, Synthesis, structural characterization, DFT studies and biological activity of Cu(II) and Ni(II) complexes of novel hydrazone, Inorg. Chim. Acta, **2018**, 480, 1–15. https://doi.org/10.1016/j.ica.2018.04.038.
38- A. Akbari, H. Ghateazadeh, R. Takjoo, B. Sadeghi-Nejad, M. Mehrvar, J.T. Mague, Synthesis crystal structures of four new biochemical active Ni(II) complexes of thiosemicarbazone and isothiosemicarbazone-based ligands: In vitro antimicrobial study, J. Mol. Struct., **2019**, 1181, 287–294. https://doi.org/10.1016/j.molstruc.2018.12.109.
39- N.C. Saha, R.J. Butcher, S. Chaudhuri, N. Saha, Synthesis and spectroscopic characterisation of new nickel (II) complexes with 5-methyl-3-formylpyrazole-3-piperidinylthiosemicarbazone (HMPz3Pi): X-ray structures of HMPz3Pi and $[Ni(HMPz_3Pi)_2]Cl_2{\cdot}2H_2O$ with indication for unusual rotation about the azomethine double bond of the free ligand on complexation, Polyhedron, **2005**, 24(9), 1015–1022. https://doi.org/10.1016/j.poly.2005.01.024.
40- S.M. Kumar, K. Dhahagani, J. Rajesh, K. Nehru, J. Annaraj, G. Chakkaravarthi, G. Rajagopal, Synthesis, characterization, structural analysis and DNA binding studies of nickel(II)–triphenylphosphine complex of ONS donor ligand – Multisubstituted thiosemicarbazone as highly selective sensor for fluoride ion, Polyhedron, **2013**, 59, 58–68. https://doi.org/10.1016/j.poly.2013.04.048.
41- P. Anitha, R. Manikandan, P. Vijayan, G. Prakash, P. Viswanathamurthi, R.J. Butcher, Nickel(II) complexes containing ONS donor ligands: Synthesis, characterization, crystal structure and catalytic application towards C-C cross-coupling reactions, J. Chem. Sci., **2015**, 127(4), 597–608. https://doi.org/10.1007/s12039-015-0811-4.
42- L. Yang, D.R. Powell, R.P. Houser, Structural variation in copper (i) complexes with pyridylmethylamide ligands: structural analysis with a new four-coordinate geometry index, τ4, Dalton Trans., **2007**, 955–964. https://doi.org/10.1039/B617136B.
43- A.S. Abdelrazeq, H.A. Ghabbour, A.A. El-Emam, D.A. Osman, S. Garcia-Granda, Synthesis and crystal structure of 3-(adamantan-1-yl)-4-(2-bromo-4-fluorophenyl)-1*H*-1,2,4-triazole-5(4 *H*)-thione, Acta Crystallogr., Sect. E: Crystallogr. Commun., **2020**, 76(2), 162–166. https://doi.org/10.1107/S2056989020000092.
44- P.P. Netalkar, S.P. Netalkar, V.K. Revankar, Transition metal complexes of thiosemicarbazone: Synthesis, structures and invitro antimicrobial studies, Polyhedron, **2015**, 100, 215–222. https://doi.org/10.1016/j.poly.2015.07.075.
45- I.M. Shahid, M. Ahmad, M. Rahisuddin, R. Arif, S. Tasneem, F. Sama, I.A. Ansari, Synthesis, crystal structures, photoluminescence, magnetic and antioxidant properties, and theoretical analysis of Zn(II) and Cu(II) complexes of an aminoalcohol ligand supported by benzoate counter anions, New J. Chem., **2019**, 43(2), 622–633. https://doi.org/10.1039/C8NJ04122A.
46- M.K. Bharty, R.K. Dani, P. Nath, A. Bharti, N.K. Singh, O. Prakash, R.K. Singh, R.J. Butcher, Syntheses, structural and thermal studies on Zn(II) complexes of 5-aryl-1,3,4-oxadiazole-2-thione and dithiocarbamates: Antibacterial activity and DFT calculations, Polyhedron, **2015**, 98, 84–95. https://doi.org/10.1016/j.poly.2015.05.045.
47- B.S. Stadelman, J.M. Murphy, A.M. Owen, R. Castro-Ramírez, H.C. Smith, C.M. Cohen, L.X. Zhang, C.A. Bayse, C. D. McMillen, N. Barba-Behrens, J.L. Brumaghim, Zinc(II) thione and selone complexes: The effect of metal redox activity on ligand-based oxidation, Inorg. Chim. Acta, **2020**, 502, 119379. https://doi.org/10.1016/j.ica.2019.119379.
48- K. Karrouchi, S.A. Brandán, Y. Sert, M.E. Karbane, S. Radi, M. Ferbinteanu, Y, Garcia, M. Ansar, Synthesis, structural, molecular docking and spectroscopic studies of (E)-N'-(4-methoxybenzylidene)-5-methyl-1H-pyrazole-3-carbohydrazide, J. Mol. Chem., **2021**, 1225, 129072. https://doi.org/10.1016/j.molstruc.2020.129072.
49- C. Ndoye, G. Excoffier, G.A. Seck, O. Diouf, I.E. Thiam, M. Sidibe, M. Gaye, Crystal structures of bis[1-(1-hydroxypropan-2-ylidene)thiosemicarbazide-κ^3 S, N, O)cobalt(III)-tetra(thiocyanato-κN) cobalt(II) methanol solvate, bis{1-(1-hydroxypropan-2-ylidene) thiosemicarbazide-κ^3 S, N, O}nickel(II) bis(thiocyanate) and (1-(1-hydroxypropan-2-ylidene) thiosemicarbazide-κ^3 S, N, O)bis(thiocyanato-κN)zinc(II), Eur. J. Chem., **2022**, 13(2), 196–205. https://doi.org/10.5155/eurjchem.13.2.196-205.2253.
50- H. Sakiyama, K. Tone, M. Yamasaki, M. Mikuriya, Electronic spectrum and magnetic properties of a dinuclear nickel(II) complex with two nickel(II) ions of C2-twisted octahedral geometry, Inorg. Chim. Acta, **2011**, 365(1), 183–189. https://doi.org/10.1016/j.ica.2010.09.005.
51- Z. Trávníček, R. Pastorek, V. Slovák, Novel octahedral nickel(II) dithiocarbamates with bi- or tetradentate N-donor ligands: X-ray structures of $[Ni(Bzppzdtc)(phen)_2]ClO_4{\cdot}CHCl_3$ and $[Ni(Bz_2dtc)_2(cyclam)]$, Polyhedron, **2008**, 27(1), 411–419. https://doi.org/10.1016/j.poly.2007.09.024.

52- K. Nakamoto, Infrared and Raman Spectra of Inorganic and Coordination Compounds, (Fifth ed.), Wiley, New York, **1986**.
53- A.K. Srivastava, K. Srivastava, P. Yadav, J. Prasad, A.K. Maurya, Synthesis, characterization, biological (in vitro) activity and electrochemical studies of mixed-ligand copper (II) and cobalt (II) complexes with picolinic acid and imides, Chem. Data Collect., **2021**, 31, 100620. https://doi.org/10.1016/j.cdc.2020.100620.
54- M.H. Sadhu, A. Solanki, S.B. Kumar, Mixed ligand complexes of copper(II), cobalt(II), nickel(II) and zinc(II) with thiocyanate and pyrazole based tetradentate ligand: Syntheses, characterizations and structures, Polyhedron, **2015**, 100, 206–214. https://doi.org/10.1016/j.poly.2015.07.067.
55- N. Gupta, R. Gupta, S. Chandra, S.S. Bawa, Magnetic, electronic and electrochemical studies of mono and binuclear Cu(II) complexes using novel macrocyclic ligands, Spectrochim. Acta, Part A, **2005**, 61(6), 1175–1180. https://doi.org/10.1016/j.saa.2004.06.038.
56- W.J. Geary, The use of conductivity measurements in organic solvents for the characterisation of coordination compounds, Coord. Chem. Rev., **1971**, 7(1), 81–122. https://doi.org/10.1016/S0010-8545(00)80009-0.